Cdc42-dependent actin dynamics controls maturation and secretory activity of dendritic cells

Anna M. Schulz,[1] Susanne Stutte,[1] Sebastian Hogl,[4] Nancy Luckashenak,[1] Diana Dudziak,[5] Céline Leroy,[1] Ignasi Forné,[2] Axel Imhof,[2] Stephan A. Müller,[4] Cord H. Brakebusch,[6] Stefan F. Lichtenthaler,[3,4,7] and Thomas Brocker[1]

[1]Institute for Immunology, [2]Adolf Butenandt Institute, and [3]Munich Cluster for Systems Neurology, Ludwig Maximilians University Munich, 80336 Munich, Germany
[4]Deutsches Zentrum für Neurodegenerative Erkrankungen, 81377 Munich, Germany
[5]Department of Dermatology, University Hospital of Erlangen, 91052 Erlangen, Germany
[6]Molecular Pathology Section, Biotech Research and Innovation Center, University of Copenhagen, 2200 Copenhagen, Denmark
[7]Neuroproteomics, Klinikum rechts der Isar, Institute for Advanced Study, Technische Universität München, 80333 Munich, Germany

Cell division cycle 42 (Cdc42) is a member of the Rho guanosine triphosphatase family and has pivotal functions in actin organization, cell migration, and proliferation. To further study the molecular mechanisms of dendritic cell (DC) regulation by Cdc42, we used Cdc42-deficient DCs. Cdc42 deficiency renders DCs phenotypically mature as they up-regulate the co-stimulatory molecule CD86 from intracellular storages to the cell surface. Cdc42 knockout DCs also accumulate high amounts of invariant chain–major histocompatibility complex (MHC) class II complexes at the cell surface, which cannot efficiently present peptide antigens (Ag's) for priming of Ag-specific CD4 T cells. Proteome analyses showed a significant reduction in lysosomal MHC class II–processing proteins, such as cathepsins, which are lost from DCs by enhanced secretion. As these effects on DCs can be mimicked by chemical actin disruption, our results propose that Cdc42 control of actin dynamics keeps DCs in an immature state, and cessation of Cdc42 activity during DC maturation facilitates secretion as well as rapid up-regulation of intracellular molecules to the cell surface.

Introduction

Dendritic cells (DCs) are positioned in tissues throughout the body, where they take up self and foreign antigens (Ag's). From there, they migrate into the T cell areas of lymph nodes (Alvarez et al., 2008) to present Ag-derived peptides in the context of major histocompatibility complex (MHC) molecules for tolerance induction or activation of Ag-specific T cells (Merad et al., 2013). Immature DCs become mature upon appropriate stimulation, a process induced by drastic changes in gene expression, protein synthesis, and surface transport to allow DCs to gain migratory and immune stimulatory properties (Merad et al., 2013). Most hallmarks of DC function and biology, such as Ag uptake, migration, and Ag presentation, are tightly regulated processes that require cell polarization and intracellular redistribution of proteins and organelles. For Ag uptake, actin polymerization generates force for the internalization of plasma membrane vesicles containing Ag's. Macropinocytosis and phagocytosis, especially, require large, actin-rich cell surface protrusions (Niedergang and Chavrier, 2004; Kerr and Teasdale, 2009). Internalized vesicles are transported along actin to Ag-processing compartments for loading onto MHC molecules and consecutive surface transport for T cell activation (Watts and Amigorena, 2000; Trombetta and Mellman, 2005; Kaksonen et al., 2006). However, the mechanisms that coordinate actin regulation during the process of DC maturation are not well described.

Rho-family GTPases (RhoGTPases) act as molecular switches, which regulate actin by cycling between inactive GDP and active GTP-bound states (Tybulewicz and Henderson, 2009). Their activity is regulated by guanine nucleotide exchange factors that induce GTP-bound states of GTPases, leading to their activation and interaction with various effectors of actin reorganization. The role of RhoGTPases in DCs has been studied initially by toxin inhibition and overexpression of dominant-negative or constitutively active mutants. Later, many of these approaches were found to have nonspecific effects on other GTPases as well (Wang and Zheng, 2007; Heasman and Ridley, 2008). Nevertheless, such experiments established the importance of GTPase cell division cycle 42 (Cdc42) in macropinocytosis and phagocytosis by DCs in some (Garrett et al.,

Correspondence to Thomas Brocker: brocker@lmu.de

A.M. Schulz's present address is Cell Biology Program, Memorial Sloan Kettering Cancer Center, New York, NY 10065.

N. Luckashenak's present address is Cidara Therapeutics, San Diego, CA 92121.

Abbreviations used in this paper: Ag, antigen; BMDC, bone marrow–derived DC; CFSE, carboxyfluorescein succinimidyl ester; CLIP, class II–associated Ii peptide; CTS, cathepsin; DC, dendritic cell; GO, gene ontology; IMDM, Iscove's modified Dulbecco's medium; ko, knockout; LC, Langerhans cell; LPS, lipopolysaccharide; MFI, mean fluorescence intensity; MHC, major histocompatibility complex; OVA, ovalbumin; qPCR, quantitative PCR; rFI, relative fluorescence intensity; TCL, total cell lysate; wt, wild type.

The Rockefeller University Press $30.00
J. Cell Biol. Vol. 211 No. 3 553–567
www.jcb.org/cgi/doi/10.1083/jcb.201503128

2000; Shurin et al., 2005b), but not all (West et al., 2000), studies. Down-regulation of Ag uptake activity during the transition from actively sampling immature DCs to uptake-inactive mature DCs has been linked to a loss of active Cdc42 during DC maturation (Garrett et al., 2000). However, receptor-mediated endocytosis depends on the cooperation of actin filaments with other proteins, such as clathrin, for internalization (Schafer, 2002; Kaksonen et al., 2006) and is therefore independent of RhoGTPases and not down-regulated in mature DCs (Garrett et al., 2000; Platt et al., 2010). This allows efficient internalization of exogenous Ag's upon binding to surface receptors during all stages of DC maturation (Allenspach et al., 2008; Platt et al., 2010).

Cdc42 has important functions in many different cell types, as it regulates cell polarity (Etienne-Manneville, 2004) and polarized secretion (Allen et al., 1998; Nobes and Hall, 1999). This allows targeted secretion of cytokines from DCs into the immune synapse and is essential for CD8 T cell priming (Pulecio et al., 2010). Using CD11c-CrexCdc42$^{fl/fl}$ mice, we showed previously that Cdc42 also controls DC migration, as Cdc42-deficient skin-resident DCs and Langerhans cells (LCs) did not efficiently migrate to draining lymph nodes (Luckashenak et al., 2013).

In this study, we found that Cdc42-deficient DCs have an MHC class II (MHCII) Ag presentation defect. Proteome analyses indicated that Cdc42 knockout (ko) DCs only inefficiently degrade the MHCII-associated invariant chain chaperone (CD74, or Ii), a defect that was mimicked by treating wild-type (wt) DCs with actin inhibitors. As a consequence, surface MHC II molecules of Cdc42 ko DCs were bound to a 12-kD Ii fragment containing the class II–associated Ii peptide (CLIP). This interferes with the loading of Ag-derived peptides and priming of Ag-specific CD4 T cells. Cdc42 ko DCs were phenotypically mature, expressing high surface levels of the DC maturation marker CD86, but lacked cytokine production. Proteome analyses indicated a loss of protein contents such as Lamp-1 (lysosomal-associated membrane protein 1) and members of the cathepsin (CTS) family, which are responsible for lysosomal Ii processing. Instead, we found cellular contents secreted spontaneously into the supernatant in the absence of Cdc42, indicating its role in controlling secretion and cell surface transport via the regulation of actin. Collectively, our results suggest that the previously reported inactivation of Cdc42 during DC maturation (Garrett et al., 2000) might facilitate rapid surface expression of maturation marker intracellular MHCII and secretion of other intracellular components important for efficient immune stimulation and T cell priming.

Results

Cdc42 is required for Ag uptake and subsequent Ag presentation to CD4 T cells

To study the role of Cdc42 in DCs in more detail, we analyzed Cdc42-deficient bone marrow–derived DCs (BMDCs) from conditional Cdc42^{flx}-Cre mice (Luckashenak et al., 2013) for their functional properties. Our previous study showed that DC-specific deletion of Cdc42 using the CD11c-Cre deleter strain led to a complete lack of Cdc42 mRNA in DCs in vivo, but only long-lived LCs and some Langerin$^+$ DCs were affected (Luckashenak et al., 2013). This either suggested differential dependencies of different DC subsets on Cdc42 or reflected the presence of residual Cdc42 protein that was still detectable in spleen DCs (Luckashenak et al., 2013). We therefore performed Western blot and quantitative PCR (qPCR) analyses to confirm a lack of Cdc42 mRNA and protein from Cdc42 ko BMDCs (Fig. 1 A). Because Ag uptake by DCs is a prerequisite for effective T cell priming, we assessed the ability of Cdc42 ko BMDCs to take up fluorescent ovalbumin (OVA) protein Ag's. Even though a comparable fraction of Cdc42 ko BMDCs and wt DCs was able to take up Alexa Fluor 488 OVA (Alexa OVA), the overall amount of internalized protein in Cdc42 ko DCs was reduced by 50% as compared with wt DCs (Fig. 1 B). In addition, when both the amount of Ag's and the incubation time were increased, Cdc42 ko BMDCs showed strongly reduced uptake as compared with wt BMDCs, even at the highest concentrations of Alexa OVA (Fig. 1 C). Furthermore, Cdc42-deficient DCs showed strongly reduced capacities to take up dextran, Lucifer yellow, or latex beads (Fig. S1, A and B). Further analyses showed that the fraction of Cdc42 ko DCs that had taken up Ag's showed normal capacities for intracellular Ag processing as measured with the fluorescence indicator DQ OVA (Fig. S1 C). These findings suggested a general deficiency for Ag uptake in the absence of Cdc42 function, confirming an earlier study (Garrett et al., 2000). As a direct consequence of such reduced Ag uptake, Cdc42 ko DCs showed a strongly reduced ability to prime OVA-specific CD4$^+$ OT-II T cells (Fig. 1 D), corroborating an earlier study using dnCdc42 proteins (Shurin et al., 2005b). However, to our surprise, when we loaded Cdc42 ko DCs externally with $OVA_{323–339}$ peptide to overcome the Ag uptake deficiencies, Cdc42 ko DCs could not efficiently present peptide Ag's for priming of OT-II T cells (Fig. 1 D). All T cell assays were performed in round-bottom plates, as described previously, so that GTPase (Rac1/2$^{-/-}$)-deficient DCs cannot properly prime CD4 T cells as a result of reduced cell–cell interactions, restricted cell motility, and other physical inhibitions (Benvenuti et al., 2004). These deficiencies were restored by physically enforcing DC–T cell interactions in round-bottom cultures, rather than in flat-bottom well plates (Benvenuti et al., 2004). As we had observed deficient T cell priming by Cdc42 ko DCs despite enforced physical interaction, we concluded that rather, Ag-mediated effects might be responsible for the observed priming deficiencies. This assumption was further supported by the fact that priming could not be substantially improved by increasing the DC/T cell ratios (Fig. S1 D).

To find the mechanisms causing diminished adenomatous polyposis coli function, we next controlled the surface expression of MHCII and CD86 (Fig. 1 E). This analysis showed that Cdc42 ko DCs did express comparable levels of surface MHC II, but that most Cdc42 ko DCs expressed high CD86 surface levels even in the absence of DC maturation stimuli such as lipopolysaccharide (LPS; Fig. 1 E). In addition, although expressing similar CD86 levels compared with mature DCs, Cdc42 ko DCs did not secrete inflammatory cytokines such as IL-6, IL-12, or TNF without further stimulation (not depicted). Another feature of DC maturation is transient loss of actin-rich podosomes to recycle actin needed for other processes, such as endocytosis (West et al., 2004). When wt DCs were plated on fibronectin-coated surfaces, they rapidly assembled actin-rich podosomes, which can be identified as phalloidin-stained punctate structures in nearly every wt DC (Fig. 1 F). After 30 min of incubation with LPS, these actin-rich structures disassemble and disappear in order to reform after 60 min in wt DCs (Fig. 1 F), as published previously (West et al., 2004). In contrast,

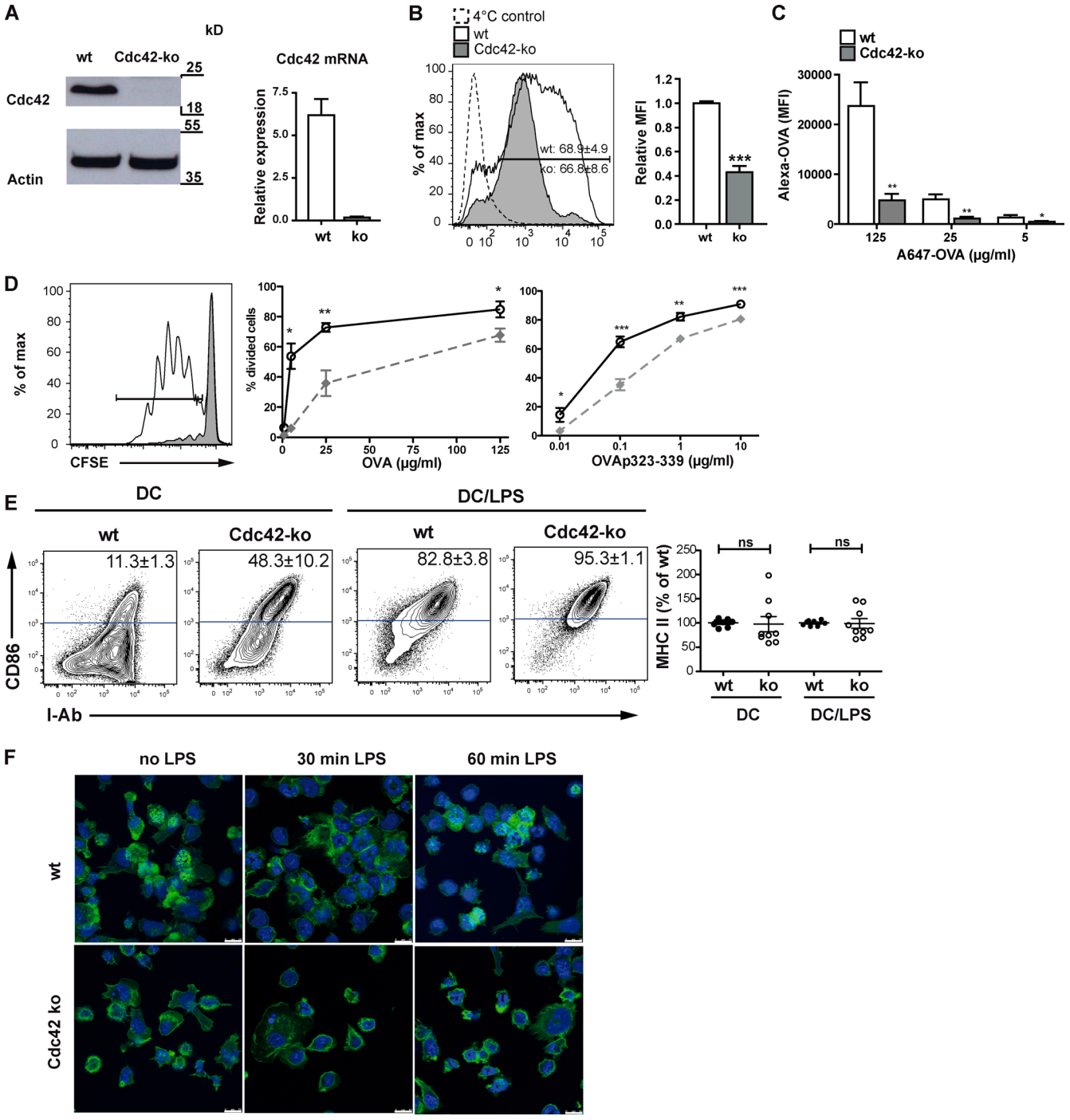

Figure 1. **Cdc42 is required for Ag uptake and subsequent Ag presentation to CD4 T cells.** (A) Cdc42 protein and mRNA are absent in Cdc42 ko BMDCs as shown by Western blotting and qPCR. Bar graph shows one representative experiment out of three with two biological replicates. (B) BMDCs were pulsed with Alexa OVA, and uptake was determined by flow cytometry. Uptake of Ag was quantified by comparing the mean fluorescence intensity (MFI) values of wt versus Cdc42 ko BMDCs. Bar graph shows pooled data from three independent experiments. (C) To evaluate a concentration-dependent effect on Ag uptake, Alexa OVA was added to BMDC cultures at different concentrations for 12 h. Cells were harvested and analyzed by flow cytometry. The bar graph shows MFI values from one experiment. $n = 3$. (D) BMDCs were pulsed with peptide-free OVA or $OVA_{323–339}$ and then co-cultured with OVA-specific CFSE-labeled OT-II T cells at the indicated concentrations. After 4 d, T cell proliferation was determined as CFSE dilution. Graphs show the percentage of divided T cells of one representative experiment. $n = 3$. (E) BMDC surface marker expression was determined by flow cytometry gating on $CD11c^+$ cells using antibodies for $I\text{-}A^b$ and CD86. MFI of MHCII expression was calculated as the percentage of MHCII MFI from wt control BMDCs. Data from three different experiments with similar outcomes were pooled ($n = 8–9$). (F) BMDCs were seeded on fibronectin-coated slides for 30 min (no LPS) and thereafter treated with 10 ng/ml LPS for 30 or 60 min. Phalloidin–Alexa Fluor 488 (green) reveals podosomes as punctate actin-rich structures in wt DCs (no LPS). As a nuclear stain, Draq5 (blue) was used. Error bars represent mean ± SEM. ns, not significant. Bars, 10 µm. *, $P < 0.05$; **, $P < 0.01$; ***, $P < 0.001$.

Cdc42 ko DCs cannot form podosomes, neither before nor after LPS stimulation (Fig. 1 F). Therefore, a lack of Cdc42 generates phenotypically mature DCs, which, although having a CD86$^+$ mature phenotype and normal MHCII levels, display an OT-II T cell–priming defect.

Cdc42 ko DCs can prime alloreactive but not Ag-specific CD4 T cells

To find out whether Cdc42 ko DCs were generally unable to prime CD4 T cells independently of Ag uptake or peptide loading, we next used Cdc42 ko and wt BMDCs from the C57BL/6 background as adenomatous polyposis coli for activation of BALB/c CD4$^+$ T cells in an alloreactive mixed lymphocyte reaction (Fig. 2 A). Here, wt and Cdc42 ko DCs could activate naive alloreactive BALB/c CD4$^+$ T cells with similar efficiency (Fig. 2 A), which argues against a general deficiency of Cdc42 ko DCs to prime CD4$^+$ T cells. To further circumvent Cdc42 ko–mediated Ag uptake deficiencies, we also targeted OVA-Ag to Dec205 receptor expressed by DCs. Ag delivery via this receptor has been reported to be RhoGTPase independent, as Dec205 is not complexed with actin (Kato et al., 2007) and is internalized efficiently in mature DCs (Platt et al., 2010), which do not express activated Cdc42 (Garrett et al., 2000). Indeed, Dec205 internalization was not compromised in Cdc42 ko DCs, as demonstrated by an internalization assay with the mAb to the Dec205 surface marker (Fig. 2 B). Cdc42 ko BMDCs showed slightly enhanced internalization capacities, which were statistically, though not significantly, different. When DCs were targeted with Dec205-OVA, Cdc42 ko DCs, in contrast with wt DCs, could not prime CD4$^+$ OT-II T cells with high efficiency (Fig. 2 C). This finding suggested that also under conditions when Ag uptake is normal, the DC priming of CD4 T cells is compromised in the absence of Cdc42. Collectively, a lack of Cdc42 generated DCs that were partially phenotypically mature, expressing high levels of CD86, which were inhibited in priming of MHCII-restricted Ag-specific CD4 T cells. This, together with the finding that the same DCs could efficiently activate alloreactive BALB/c CD4 T cells, suggests that Cdc42 controls Ag processing itself, rather than DC–CD4 T cell interaction.

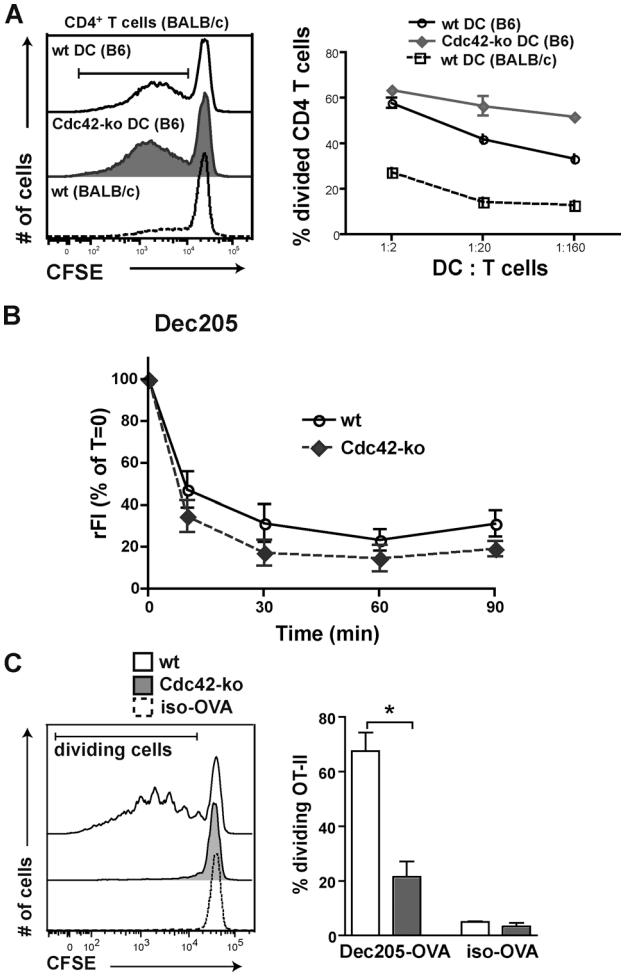

Figure 2. **Cdc42 controls priming of Ag-specific, but not alloreactive, CD4 T cells.** (A) wt or Cdc42 ko BMDCs (on B57BL/6 background) and BMDCs (BALB/c) were co-cultured with CFSE-labeled BALB/c CD4$^+$ T cells at indicated DC/T cell ratios for 4 d. T cell proliferation of CFSE-labeled CD4$^+$ T cells was analyzed by flow cytometry, and the graph shows the percentage of dividing CD4$^+$ T cells of one representative experiment out of two. $n = 2$. (B) Internalization of the Dec205 surface receptor was tested with specific antibody in wt and Cdc42 ko BMDCs by detection of remaining antibody at the indicated times. The graph shows rFI values on CD11c$^+$ cells as percentages of time zero from two pooled experiments. $n = 4$. (C) BMDCs were incubated with Dec205-OVA and subsequently co-cultured with CFSE-labeled OT-II cells. Proliferation of T cells was measured by flow cytometry (left), and the frequency of divided T cells was determined (right). As a control, isotype antibody conjugated to OVA (iso-OVA) was applied. One representative experiment of two is shown, each with two mice per group. *, $P < 0.05$.

Cdc42 ko BMDCs have altered protein contents

To further investigate the basis for this MHCII presentation deficiency, we performed an unbiased proteomic screen comparing wt and Cdc42 ko DCs. This analysis quantified 2,897 proteins, which were identified by at least two unique peptides each, with 7% of the proteins being more than twofold differentially regulated (Proteomics Identifications [PRIDE] partner repository, dataset identifier PXD001934). Cdc42 protein levels were reduced 4.5-fold, confirming the knockout of the protein (Fig. 3 A). We next used a gene ontology (GO) analysis and found that proteins associated with the cellular component lysosome (GO:0005764) accumulated significant changes in Cdc42 ko DCs. 20% of the 388 proteins listed under this term could be identified in our screen. Of those, 16% were more than twofold up- or down-regulated in the absence of Cdc42 (Table S1). Lysosomal proteins such as Lamp-1 and different CTSs were present in reduced amounts when Cdc42 was absent (Fig. 3 A). In addition, among the regulated proteins, several microtubule- and actin-binding proteins were present at increased amounts in the absence of Cdc42 ko (Fig. 3 A; and Tables S2 and S3). Functional annotation clustering by the Database for Annotation, Visualization, and Integrated Discovery (DAVID; Huang et al., 2009a,b) revealed five clusters with an enrichment score larger than one (Tables S4 and S5). Among those, the second cluster includes 15 lysosomal proteins, of which 12 showed to be down-regulated, and clusters three and four are linked to immune response. Clustering by DAVID is a rough analysis of the data. Nevertheless, the functional cluster analysis supports the findings that cell morphogenesis, immune response ability, and lysosomes are altered in the absence of Cdc42.

Immunofluorescence staining with phalloidin revealed large numbers of aggregated phalloidin-positive F-actin structures in Cdc42 ko BMDCs, but not in wt DCs (Fig. 3 B),

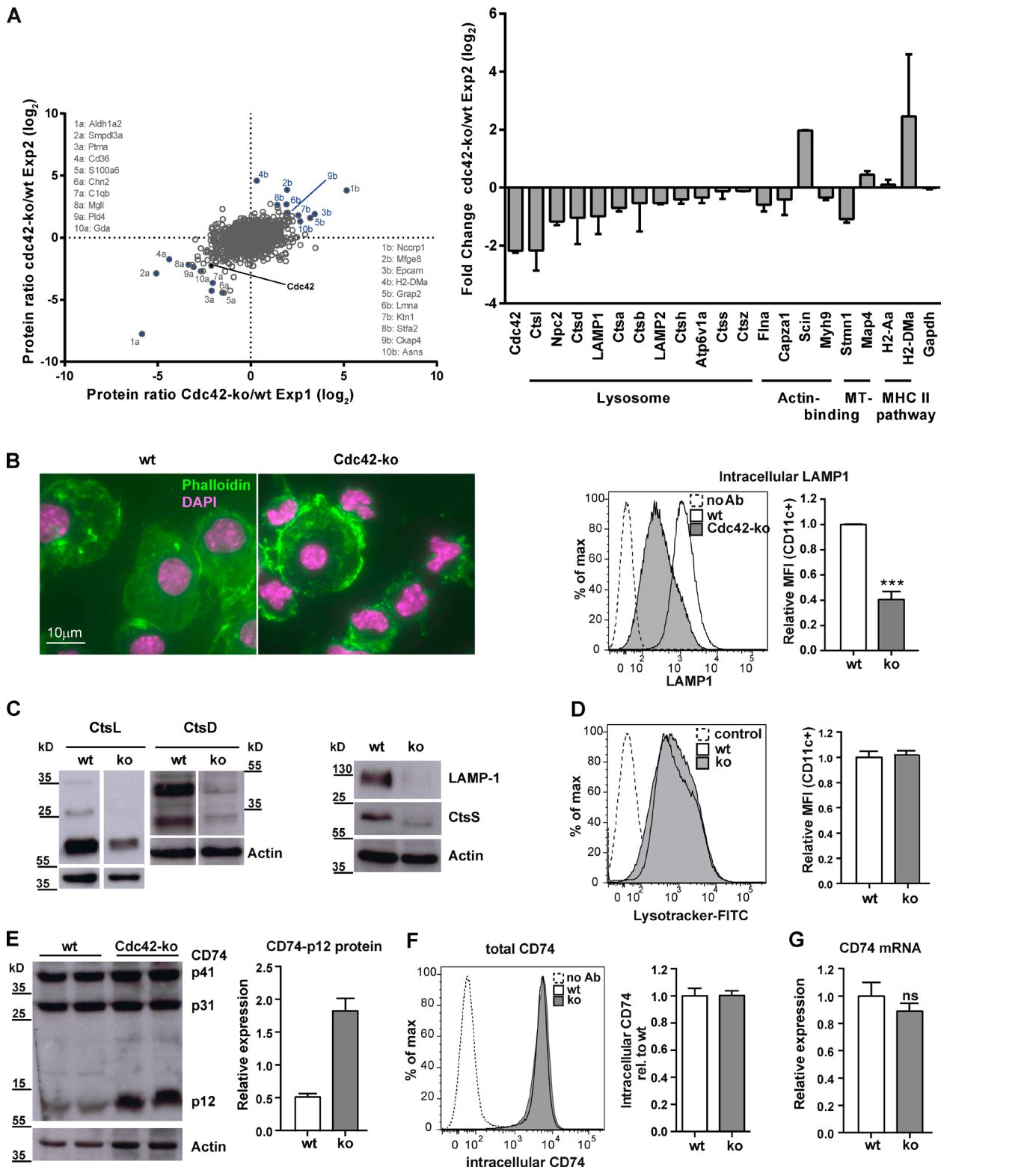

Figure 3. **Cdc42 ko BMDCs lack lysosomal proteases and accumulate the p12 degradation intermediate of Ii.** (A) A quantitative proteomics screen from wt and Cdc42 ko BMDCs revealed differences in the expression of lysosomal proteins. The diagram shows the distribution of the relative ratios of protein levels between Cdc42 ko and wt cells for proteins, which were quantifiable in both biological replicates. The histogram shows the mean fold change values with SEM of selected proteins from combined data of two independent representative experiments out of four repeats. For the experiments shown, $n = 2$. (B, left) Microscopic analysis of cytospins of wt and Cdc42 ko BMDCs using phalloidin–Alexa Fluor 488 for detection of actin cytoskeleton and nuclear staining with DAPI (pink). The experiment was performed in triplicates. BMDCs were fixed, stained intracellularly with LAMP-1 antibody, and analyzed by flow cytometry (right). MFIs are depicted as MFI of $CD11c^+$ cells relative to wt/DC as 100%. The histogram shows pooled data from two independent experiments. $n = 3$. ***, $P < 0.001$. (C) BMDC TCLs were analyzed by Western blotting using specific antibodies for LAMP-1 and the CTSS, CTSL, and CTSD. Actin was used as a loading control. Each Western blot shows one representative out of at least three independent experiments. (D) LysoTracker

whereas FACS analysis (Fig. 3 B, right) with LAMP-1–specific mAb confirmed reduced LAMP-1 levels in Cdc42 ko DCs.

As CTSs control MHCII presentation by proteolytic cleavage of the Ii CD74 chaperone (Hsing and Rudensky, 2005), we further verified these results by Western blot analyses and could confirm the lower content of LAMP-1, CTSS, CTSL, and CTSD proteins in Cdc42 ko BMDCs (Fig. 3 C). To find out whether the reduction of lysosomal proteins was caused by a general lack of lysosomes in Cdc42-deficient DCs, we labeled live cells with LysoTracker probes (Fig. 3 D). However, Cdc42 ko DCs showed comparable amounts of lysosomes as determined with LysoTracker stainings (Fig. 3 D). In late endosomal compartments, CTSs are involved in important processing steps (Hsing and Rudensky, 2005) that guarantee degradation of Ii to generate the residual CLIP, which occupies the peptide-binding groove of MHCII molecules (Neefjes et al., 2011). The CLIP peptide, in turn, can be exchanged against appropriate Ag peptides for presentation to CD4 T cells. Because we found CTS proteins strongly down-regulated in Cdc42 ko cells (Fig. 3, A and B), we next investigated whether Ii processing was affected in the absence of Cdc42. To visualize Ii degradation intermediates, we used an antibody specific for the cytoplasmic N-terminal part of Ii (clone In-1) to analyze total cell lysates (TCLs) by Western blotting (Fig. 3 E). This antibody revealed 41-kD, 31-kD, and 12-kD degradation intermediates of Ii (Fig. 3 E). The 12-kD Ii fragment was detectable only at low abundance in wt DCs (Fig. 3 E), but at much higher levels in Cdc42 DCs (Fig. 3 E). In several experiments, we could also detect a strong accumulation of the higher molecular weight isoforms Ii-p41 and Ii-p31 in addition to Ii-p12 (Fig. S2). Such accumulation was not the result of transcriptional regulation because the total intracellular amount of Ii as detected by intracellular staining and flow cytometry (Fig. 3 F), as well as the amount of Ii-mRNA in Cdc42 ko DCs, was unchanged compared with wt DCs (Fig. 3 G). We therefore concluded that the observed differences in Ii proteins were caused by differential degradation of Ii protein, possibly because of reduced CTS contents in the absence of Cdc42.

Ii–MHCII complexes accumulate on the surface of Cdc42 ko DCs

Normal turnover of Ii may also include a passage via the plasma membrane (Wraight et al., 1990; Neefjes et al., 2011). From there, Ii–MHCII complexes are internalized for further transport by AP2- and clathrin-dependent mechanisms to endocytic compartments, where processing and Ag loading occurs (Dugast et al., 2005; McCormick et al., 2005). Because we found a defect in Ii processing in Cdc42 ko cells, we next assessed how many surface MHCII molecules were still complexed to Ii. To this end, we used an antibody (clone 15G4) recognizing an epitope of Ii bound to MHCII I-A^b (Beers et al., 2005). We performed a FACS analysis and stained for total I-A^b and 15G4 at the cell surface of DCs. This analysis revealed that a higher percentage of immature as well as mature Cdc42 ko DCs showed highly increased 15G4 surface staining (Fig. 4 A). To determine how many I-A^b molecules were occupied by Ii, we calculated the ratio of 15G4 to total I-A^b (Fig. 4 B). Cdc42 ko DCs showed approximately twofold higher 15G4/I-A^b ratios on their cell surface than wt DCs, suggesting that Cdc42 ko DCs express a large fraction of MHCII molecules, where Ii occupies the Ag peptide–binding grooves (Fig. 4 B). Notably, wt DCs also increased their surface levels of Ii-complexed MHCII upon maturation, probably because of LPS stimulation–induced export of cytoplasmic MHCII compartments (MIICs), which contain both MHCII–peptide complexes as well as immature Ii–MHCII complexes (Fig. 4, A and B). In contrast, a lack of Cdc42 allows contents from these compartments to accumulate at the cell surface even without additional inflammatory DC maturation stimuli.

As Cdc42-regulated actin polymerization has also been suggested to control clathrin-mediated endocytosis (Zhang et al., 1999; McGavin et al., 2001; Qualmann and Mellor, 2003), a deficiency in this mechanism might contribute to accumulation of Ii–MHCII molecules on the DC surface. We therefore analyzed the capacities of wt or Cdc42 ko DCs to internalize Ii–MHCII molecules (Fig. 4 C). In contrast to wt DCs, Cdc42 ko DCs internalized the Ii–MHCII complexes only with low efficiency (Fig. 4 C). This suggests that Cdc42 is not only required for Ii processing, but also for its internalization. Together, these defects lead to Ii–MHCII accumulation on the cell surface of Cdc42 ko DCs and may contribute to their poor capacity to stimulate Ag-specific $CD4^+$ OT-II cells (Fig. 1 D).

It has been reported previously that in the Ii, CD74 associates with myosin II, a motor protein that binds actin and is required for DCs to migrate through tissues (Lämmermann et al., 2008). Defective degradation of CD74 can therefore impair the migratory capacities of DCs via myosin II (Faure-André et al., 2008). As we have published previously that Cdc42 ko LCs show defective migratory capacities, we wondered whether the accumulation of Ii on the surface of Cdc42 ko DCs would lead to a sequestration of myosin II to the periphery of Cdc42 ko DCs. Confocal analysis of DCs showed a localization of myosin II to the periphery of DCs in ~40% of Cdc42 ko DCs and 1.7% of wt DCs (Fig. 4 D). Collectively, our results suggest that Cdc42 deficiency leads to accumulations of Ii–MHCII complexes at the surface of DCs, which are consequently associated with myosin II.

Actin dynamics are important for efficient Ii degradation

To find out whether Cdc42-dependent actin dynamics might be responsible for accumulation of Ii–MHCII complexes at the surface of Cdc42 ko DCs, we next studied the consequences of actin disruption for Ii degradation. To this end, we used latrunculin B (LatB) and cytochalasin D (CytD), two different actin inhibitors that interfere with F-actin polymerization. First, we analyzed cell surface expression of MHCII and Ii. Both actin inhibitors LatB and CytD induced surface up-regulation of I-A^b as well as Ii–I-A^b complexes on wt DCs (Fig. 5 A). In contrast,

was added to the cells to evaluate the amount of total lysosomal content and analyzed by flow cytometry. Bar graph shows one representative experiment. $n = 2$. (E) BMDC lysates were analyzed by Western blotting using an antibody specific for Ii (clone In-1) that recognizes a 41- and 31-kD isoform as well as a 12-kD processing intermediate of CD74. Actin was used as a loading control. Bar graph shows a quantification of the Western blotting shown ($n = 2$), which was one of more than three experiments with similar outcomes. (F) To determine the total levels of CD74, BMDCs were stained intracellularly with CD74-specific mAb and analyzed by flow cytometry. (G) qPCR was performed using CD74-specific primers and cDNA from wt and Cdc42 ko BMDCs. Relative expression levels of CD74 mRNA are from three combined experiments, each with DCs from a minimum of two mice per group. ns, not significant.

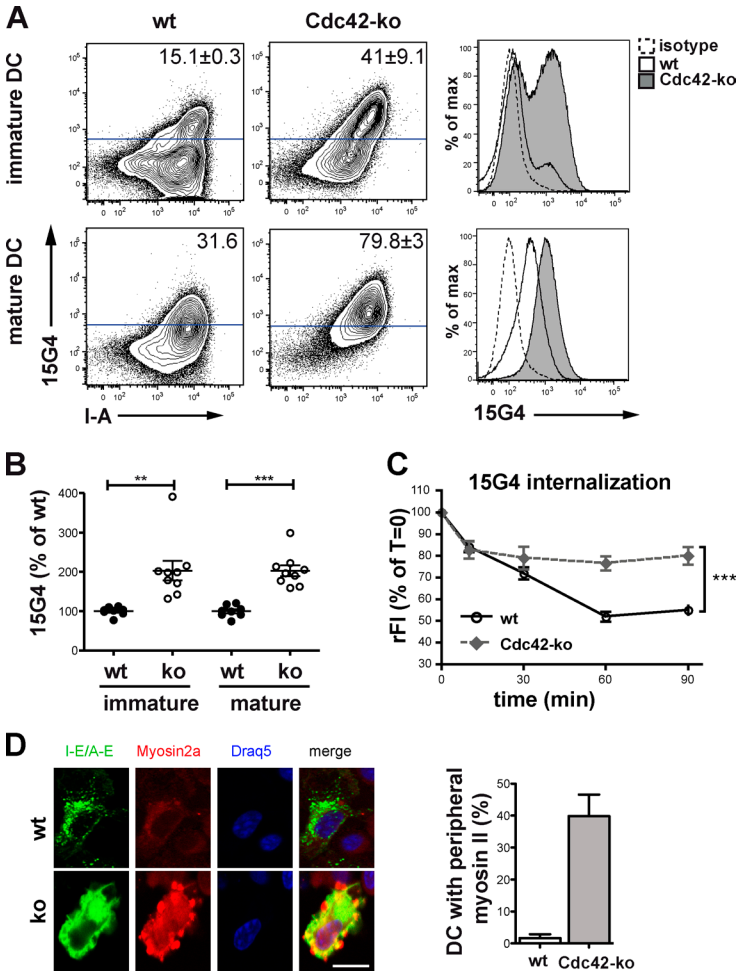

Figure 4. **Ii-complexed MHCII accumulates at the cell surface of Cdc42 ko BMDCs.** (A) Steady-state (immature) and LPS-treated (mature) CD11c+ BMDCs were analyzed by flow cytometry for total surface I-Ab and Ii bound to I-Ab (15G4). Data shown are from a single representative experiment out of more than four repeats. For this experiment, *n* = 3. (B) MFI values obtained from flow cytometry of A were used to calculate the ratio of Ii-bound I-Ab (15G4) to total surface I-Ab in wt versus Cdc42 ko BMDCs. Graph shows pooled data from three independent experiments with similar outcomes. *n* = 8–9. (C) Internalization of the 15G4 antibody was measured by detection of the remaining 15G4 antibody at the indicated times. The graph shows rFI values on CD11c+ cells as percentages of time zero. Data are from two pooled experiments. *n* = 4. (D) Cdc42 ko and wt BMDCs were seeded on fibronectin-coated slides, fixed, and stained for myosin II, I-E/A-E, and nuclei (Draq5). Bar, 10 µm. A total of 225 DCs on 24 slides were analyzed for the colocalization of MHCII and myosin II. Bar graph shows the percentage of DCs with peripheral myosin II localization in Cdc42 ko and wt DCs. Error bars represent mean ± SEM. **, P < 0.01; ***, P < 0.001.

nocodazole (Noco) and concanamycin B (ConB) did not show effects on the surface I-A or Ii in DCs (Fig. 5 A), indicating that neither microtubules nor the proton pump, which regulates endosomal acidification, play roles during this process. Interestingly, LatB- and CytD-treated wt DCs also up-regulated CD86 (Fig. 5 B), similar to Cdc42 ko DCs (Fig. 1 E). In contrast to LPS-treated controls, LatB- or CytD-treated DCs did not up-regulate CD86-specific mRNA (Fig. 5 B), suggesting that CD86 surface up-regulation by inhibition of the actin cytoskeleton (Fig. 4 B) or Cdc42 deficiency (Fig. 1 E) occurred independently of de novo gene transcription. Therefore, the up-regulation of Ii–I-Ab and CD86 on immature DCs can be enforced by a chemical inhibition of actin dynamics or a deficiency for Cdc42. We further confirmed on supernatants from these cultures that LatB or CytD treatment did not cause functional DC maturation, as none of the inhibitor-treated DCs produced any inflammatory cytokines such as IL-12 p70, TNF, IFN-γ, MCP-1, IL-10, or IL-6 (Fig. S3). These findings suggest that the regulation of surface Ii–I-Ab complexes was induced most likely by interference with actin dynamics and independently from functional DC maturation, as for example obtained with LPS.

We next compared CTSL and CTSS expression and Ii processing in inhibitor-treated BMDCs to investigate a possible link between Ii processing and actin dynamics. Actin inhibitor treatment of wt DCs induced a loss of CTSL and CTSS from DC lysates (Fig. 5 C), similar to what we observed in Cdc42 ko DCs (Fig. 3, A and B). Consequently, an increase of the Ii-p12 fragment could be found upon actin inhibition with CytD (Fig. 5 C). In contrast, interrupting the microtubule network by Noco treatment did not show any effects on Ii-p12 degradation. Also, the effects of the V-ATPase–disrupting drug ConB on Ii-p12 degradation was modest as compared with CytD treatment and did not involve a decrease in cellular CTSS or CTSL levels (Fig. 5 C). Most likely, altered pH of late endosomes resulting from ConB treatment could cause slightly increased Ii-p12 levels because of inefficient activation of cysteine proteases, which are active only at an acidic pH (Turk et al., 2012). To clarify whether Cdc42 deficiency induced a complete loss of cellular proteins, we treated Cdc42 ko DCs with the same inhibitors (Fig. S4). LatB- or CytD-treated Cdc42 ko DCs could further decrease CTSL contents (Fig. S4). As a consequence, processing of Ii-p12 was further reduced, resulting in additional accumulation of Ii-p12 (Fig. S4). Therefore, although Cdc42 ko caused a strong reduction of CTSL, residual levels of this enzyme were still present (Fig. 3 C), which could be further decreased by chemical actin inhibition.

We wondered whether the loss of intracellular levels of CTS proteins upon treatment of cells with actin inhibitors would result in their secretion and analyzed supernatants from DC cultures. We found that CTSL was secreted in high amounts upon LatB and CytD treatment of wt DCs, whereas neither ConB nor Noco treatment showed similar effects (Fig. 5 D). In contrast, it was impossible to detect CTSS in the supernatant (not depicted), probably because of a relatively low abundance in the cell and/or protein instability. These findings indicated that inhibition of the actin dynamics led to accumulation of cellular

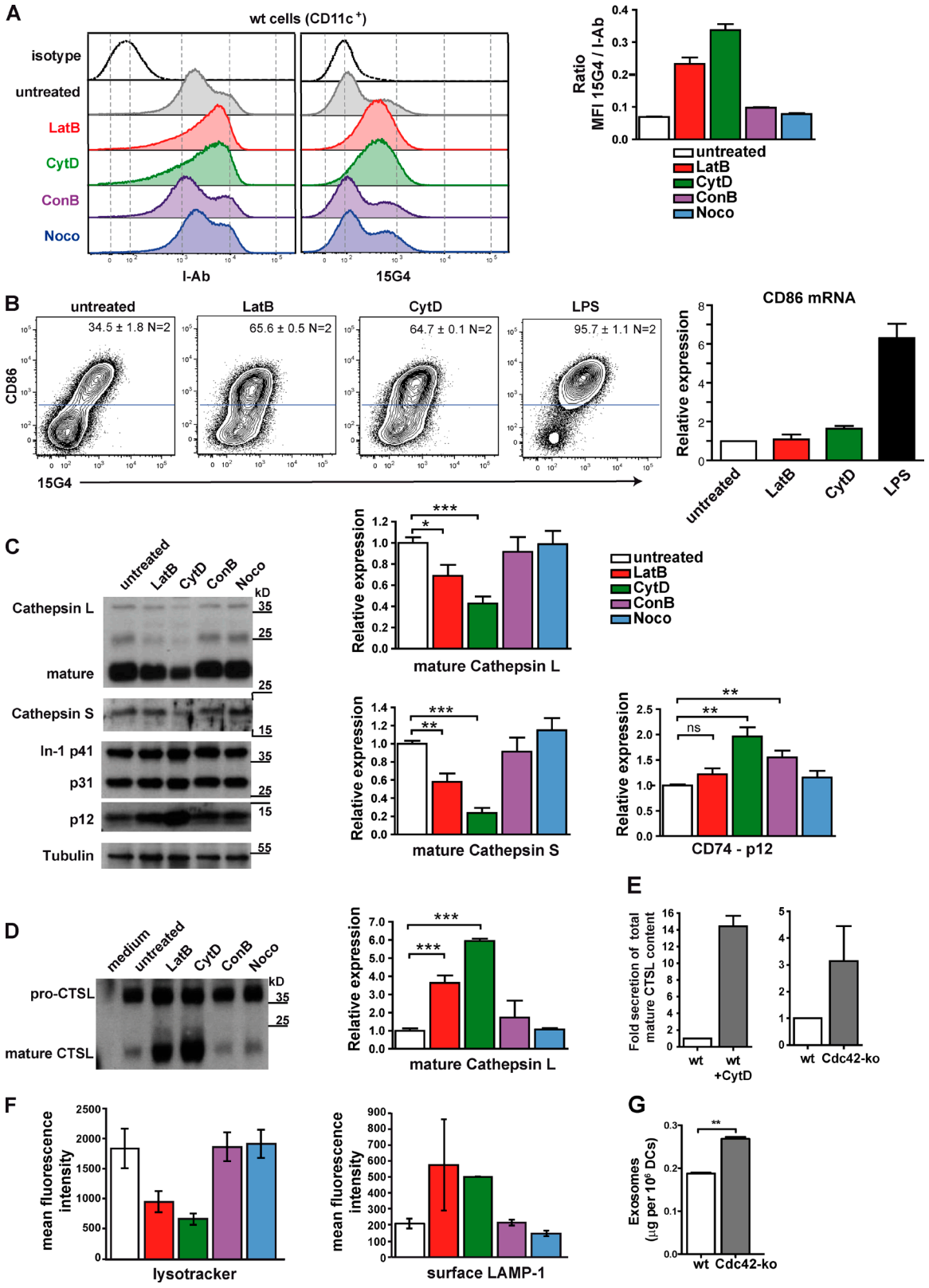

Figure 5. **Actin inhibition in wt BMDCs causes effects similar to Cdc42 deficiency.** (A) wt BMDCs were treated with actin inhibitors (LatB and CytD), V-ATPase inhibitor ConB, or microtubule inhibitor Noco overnight, or left untreated. Total surface I-A^b (clone AF6-120.1) and Ii-complexed I-A^b (clone 15G4) were analyzed by flow cytometry by gating on $CD11c^+$ cells. Bar graphs show the ratio of MFI 15G4/total surface I-A^b of one representative experiment out of three. *n* = 2. (B) wt BMDCs were treated with inhibitors as mentioned in A, and $CD11c^+$ DCs were analyzed for surface expression of $15G4^+$ Ii–MHC II complexes and CD86. Bar graph shows the results from qPCRs on cDNA prepared from these differentially treated DCs with primers specific for CD86. Data are from two combined experiments. *n* = 3. (C) TCLs were analyzed by Western blotting for CTSL, CTSS, and Ii (clone In-1). Tubulin served as a loading control. Bar graphs show a quantification of protein expression levels from two independent experiments (*n* = 4) normalized to tubulin. (D) Supernatants

proteins and enzymes in the supernatants. When total cellular content of CTSL was compared with the secreted CTSL, we found enhanced secretion in both CytD-treated wt and untreated Cdc42 ko DCs (Fig. 5 E). These data suggest that inhibition of actin dynamics either by chemical inhibitors or by Cdc42 deficiency leads to surface up-regulation of Ii–MHCII complexes and CD86 (Fig. 5 B) and enhanced secretion of mature CTSL into the culture supernatants (Fig. 5, D and E). The fact that secretion affected predominantly the mature form of CTSL upon actin inhibition or Cdc42 deficiency (Fig. 5, D and E) suggested that mostly post-Golgi compartments were secreted, where mature CTSL but not pro-CTSL forms are present (Katunuma, 2010). To further study chemical inhibition of actin in DCs, we analyzed the presence of lysosomes and surface expression of LAMP-1 (Fig. 5 F). Both actin inhibitors LatB and CytD, but not the other chemical compounds tested, could substantially decrease the staining with LysoTracker as a marker for lysosomal content (Fig. 5 F, left). As a result of such acute actin inhibition, we could observe a concomitant up-regulation of LAMP-1 to the cell surface (Fig. 5 F, right).

DCs also secrete exosomes, which are vesicles formed inside late endocytic compartments such as multivesicular bodies (Zitvogel et al., 1998). As our experiments had suggested enhanced secretion of proteins by Cdc42 ko DCs, we wondered whether they would also show increased secretion of exosomes. We therefore measured the amount of exosomes secreted by identical numbers of cultured DCs (Fig. 5 G). Indeed, Cdc42 ko DCs secreted significantly more exosomes than wt DCs (Fig. 5 G). The protein composition of exosomes derived from Cdc42 ko DCs mirrored their TCLs with elevated levels of CD74-p41, -p31, and -p12 and reduced CTSL (Fig. S5). Also, CD9 and MFG-E8, proteins typically enriched in exosomes as compared with lysates, were present in higher amounts (Fig. S5). Collectively, our data indicate that Cdc42-controlled actin dynamics regulates secretion of proteins as well as exosomes in DCs.

Discussion

We have previously shown that Cdc42 controls migration of LCs and dermal DCs to draining lymph nodes (Luckashenak et al., 2013). The present study aimed at understanding if and how Cdc42 controls other DC properties such as Ag uptake, presentation, and maturation. Our results suggest a role for Cdc42 in MHCII loading and trafficking based on three observations: Cdc42 ko BMDCs showed (1) low levels of the protease CTSS that conducts the final step of Ii-p12 processing, (2) an intracellular increase of the smallest degradation intermediate of Ii, Ii-p12, and (3) an accumulation of Ii-bound MHCII and CD86 on the surface. These new findings might also help to explain migratory deficiencies of Cdc42 ko DCs previously observed (Luckashenak et al., 2013), as CD74 was identified to associate with myosin II in DCs and inhibit DC migration (Faure-André et al., 2008). Therefore, accumulation of Ii as a result of Cdc42 deficiency leads to accumulation of Ii-bound myosin II in the periphery of DCs, which acts as a brake for DCs (Lukacs-Kornek and Turley, 2008). Together, this generated MHCII molecules, which were preoccupied with Ii at the cell surface of Cdc42 ko BMDCs. As a consequence, Cdc42-deficient DCs show a low efficacy of MHCII loading with antigenic peptides, resulting in inefficient Ag-specific CD4 T cell priming.

Prevention of peptide binding by CLIP-containing Ii was shown initially in Ii-deficient mice (Bodmer et al., 1994). Although Ii blocks access to MHCII for the majority of peptides, some Ag's can bind to MHCII after translocation into the endoplasmatic reticulum (Tewari et al., 2005). In addition, the cytoplasmic tail of Ii contains sorting motives responsible for directing MHCII molecules to late endosomal MIICs (Landsverk et al., 2009), either from the trans-Golgi network or from the plasma membrane (Neefjes et al., 2011). Immature DCs seem to preferentially use the latter route (Dugast et al., 2005; McCormick et al., 2005), whereas mature DCs sort MHCII directly from the trans-Golgi (Santambrogio et al., 2005). Internalization of Ii–MHCII from the plasma membrane was strongly decreased in the absence of Cdc42, which, together with enhanced secretory activity of Ii–MHCII and CD86-containing compartments, probably contributed to an accumulation of surface Ii–MHCII. Internalization of MHCII molecules from the plasma membrane in immature DCs is regulated by oligoubiquitination of the MHC II β chain (van Niel et al., 2006). This mechanism depends on Ii processing, as internalization of MHCII was only observed after Ii was fully processed by lysosomal proteases (van Niel et al., 2006). Thus, incomplete processing of Ii-p12 into CLIP may prevent the exposure of MHCII-β to the ubiquitination machinery, thereby stabilizing MHCII and Ii–MHCII at the cell surface. Therefore, although we do not have direct evidence, altered ubiquitination of MHCII and CD86 might also contribute to the accumulation of the molecules on the cell surface. In addition, it has been demonstrated that clathrin and the adapter protein AP2 are involved in Ii down-regulation from the cell surface, and inhibition of clathrin-mediated down-regulation of Ii–MHCII complexes led to an increase in surface expression of Ii and a decrease of peptide-loaded MHCII complexes on the surface (McCormick et al., 2005). Hence, the accumulation of surface MHCII–Ii-p12in Cdc42 ko DCs could also represent a trafficking defect, especially because Cdc42 effector proteins were shown to be associated with clathrin-mediated endocytosis (Anitei and Hoflack, 2011) and our own internalization assays revealed a decreased internalization rate of MHC. Although overall MHCII levels at the cell surface of immature Cdc42 ko BMDCs were not elevated, we found an increased proportion of Ii–MHCII complexes. As chemical actin inhibition also blocked internalization of MHCII in wt DCs (unpublished data), both Cdc42 and functional actin dynamics are important for the internalization of MHCII from the plasma membrane. Our data suggest that Cdc42 controls Ii transport from the surface to endosomal compartments, as measured by reduced internalization of Ii–MHCII complexes.

of these samples, including Cdc42 ko culture supernatants, were analyzed by Western blotting. For this purpose, equal amounts of protein were loaded, and a medium was used as a negative control. Bar graph shows a quantification of protein expression levels from two independent experiments (n = 2–4) normalized to actin. (E) Bar graphs show fold secretion of total 20-kD CTSL content taking into account intracellular CTSL and extracellular CTSL that was present in culture supernatants. (F) Bar graphs show MFI of LysoTracker (left) or surface LAMP-1 expression (right) as determined by FACS analysis of wt DCs treated with various inhibitors as described in A. (G) Bar graph shows the total amount of exosomes secreted by wt versus Cdc42 ko BMDCs normalized to seeded cell numbers (24 h before exosome purification) from two independent experiments. n = 4. Error bars represent mean ± SEM. ns, not significant. *, $P < 0.05$; **, $P < 0.01$; ***, $P < 0.001$.

DC maturation results in up-regulation of surface MHC molecules, co-stimulatory molecules, cytokine, and chemokine receptors, as well as secretion of cytokines that contribute to efficient priming of T cells. Loss of Cdc42 has been reported to decrease the capacity of DCs to form functional DC–T cell synapses because of cytoskeletal defects (Benvenuti et al., 2004) as well as a deficiency to secrete intracellular stores of IL-12 in a polarized fashion toward the immunological synapse (Pulecio et al., 2010). Although DC–T cell contact can be enforced by appropriate experimental conditions (Benvenuti et al., 2004), IL-12 release by DCs is a signal promoting full activation and survival of activated T cells. Our own data confirmed that IL-12 secretion was indeed significantly reduced in Cdc42 ko DCs (60 ± 7.2% of wt; $n = 8$, **, $P < 0.001$; unpublished data), as measured from supernatants of LPS-treated Cdc42 ko BMDCs. Also, other cytokines were reduced in supernatants of LPS-treated Cdc42 ko BMDCs (IL-6, 39 ± 5.8% of wt and TNF, 44 ± 5.4% of wt; $n = 8$, ***, $P < 0.0001$; unpublished data). These results suggest that in Cdc42 ko DCs, multiple pathways, including the production and release of inflammatory cytokines, are defective.

DC maturation is accompanied by substantial rearrangements of the actin cytoskeleton (West et al., 2004), leading to a shutdown of endocytosis of soluble Ag's (Garrett et al., 2000) and an enhanced transport of vesicles to the cell surface. Although human LCs seem to up-regulate Cdc42 activity (Jaksits et al., 2004), it has been reported that Cdc42 activity does not increase in mature DCs (Kamon et al., 2006), but rather gradually decrease upon DC maturation (Garrett et al., 2000). As a result, immature DCs with high Cdc42 activity show a high potential of Ag uptake, whereas mature DCs with lower Cdc42 activity have low Ag uptake potential to avoid continued uptake of irrelevant Ag's (Garrett et al., 2000). Although some studies showed different results, as mutant Cdc42-transfected spleen DCs did not show a significant defect in Ag uptake (West et al., 2000), our findings in Cdc42 ko DCs confirmed that Cdc42 controls Ag uptake and are in agreement with previous studies showing that most pathways of Ag uptake required Cdc42 functions (Garrett et al., 2000; Shurin et al., 2005a). Our own findings on spleen DCs from Cdc42 ko mice showed highly significantly reduced uptake capacities of apoptotic material and weaker, but statistically significant, effects on uptake of soluble OVA (unpublished data). Although the Cdc42 ko efficiency was not 100% in spleen DCs (Luckashenak et al., 2013), these reductions argue for Cdc42 control of Ag uptake in both BMDCs and spleen DCs. Also, other in vivo models of conditional Cdc42-deficient mice previously showed different efficiencies of Cdc42 deletion depending on the promoter used to drive Cre expression and the time point of efficient deletion. For example, although CD19-Cre led to Cdc42 ko B cells with only mild phenotypes (Guo et al., 2009), the usage of *mb1*Cre mice, which leads to more efficient deletion early during B cell development, had drastic effects on B cell differentiation and immunity (Burbage et al., 2015). Also, in B cells, Cdc42 was shown to control polarized secretion of cellular content for Ag extraction and processing (Yuseff et al., 2011) and B cell differentiation and immunity (Guo et al., 2009; Burbage et al., 2015) when efficiently deleted. However, although the ko efficiency in DCs of lymph nodes and spleens of CD11cCrexCdc42$^{fl/fl}$ was complete on the mRNA level, we found stable residual Cdc42 protein in ex vivo isolated Cdc42 ko DCs (Luckashenak et al., 2013). This made reliable in vivo studies in Cdc42 ko DCs in vivo not possible.

Active Cdc42 controls the integrity of cortical actin, which has a barrier effect to minimize inadvertent secretion (Orci et al., 1972). It has been shown previously in other cell types that secretion of vesicles might require reorganization of the continuity of the cortical actin network, and that F-actin disassembly can lead to the presence of aggregates in the cell periphery and interior and lead to enhanced secretion of cell contents (Burgoyne et al., 1989). When F-actin levels are low enough to allow passage of vesicles through the cortical actin, secretion is enhanced (Wollman and Meyer, 2012). Therefore, the loss or inactivation of Cdc42 upon DC maturation might cause such a redistribution of actin, weaken the cortical actin structure, and allow secretion of intracellular vesicles. We found up-regulation of Ii–MHCII complexes in Cdc42 ko DCs being enhanced. MHCII molecules in DCs target late endosomal MIICs (Engering et al., 1997; Kleijmeer et al., 1997; Inaba et al., 2000), and newly formed immunogenic MHCII–peptide complexes are subsequently transported from there to the cell surface of DCs (Boes et al., 2002; Chow et al., 2002). Also, the DC maturation marker CD86 was up-regulated on the surface of Cdc42 ko DCs. CD86 is transported to the cell surface from intracellular storage compartments upon DC maturation (Smyth et al., 1998, 2005). In human DCs, these CD86-containing cytoplasmic vesicles are distinct structures different from the Golgi apparatus, MIICs, or endocytic vesicles (Smyth et al., 2005), indicating that not only MIIC, which contain MHCII, Ii, and CTS in activated DCs (Lautwein et al., 2002), but also other vesicles are retained and controlled by cortical actin integrity. Therefore, the down-regulation of active Cdc42 by maturing DCs (Garrett et al., 2000) might be a key mechanism by DCs to control the maturation process by (a) stopping of Ag uptake (Garrett et al., 2000), (b) fast up-regulation of cytoplasmic co-stimulatory molecules MHCII, and (c) facilitation of cytokine secretion. Ag uptake by macropinocytosis and secretion are linked in DCs, as enhanced macropinocytosis is accompanied by enhanced exocytosis of endocytic vesicles to prevent overload of cells with macropinosomes (Falcone et al., 2006). We found that Cdc42 deficiency induced both, decelerated micropinocytosis, and enhanced exosome secretion. However, it is currently unclear to what extent defective cortical actin or other factors are responsible for enhanced exosome secretion by Cdc42 ko DCs. We also found in the proteome screen Rab27a, a regulator of exocytosis being increased (Tables S1 and S5), which might enhance exocytosis. Therefore, the loss of active Cdc42 in mature DCs might also contribute to enhanced exosome secretion. Inhibition of Cdc42 function in β-pancreas cells by glucose also induced the loss of cortical actin and exocytosis of granules (Nevins and Thurmond, 2003). As observed recently by superresolution microscopy, the cortical action mesh also opens up specific holes in natural killer cells to facilitate secretion of granules (Brown et al., 2011).

Although our proteomic analysis of Cdc42 ko DCs was performed with lysate from whole DCs and not with purified lysosomes, the cumulative change in lysosomal contents argue that the lysosomal/late endosomal compartment was specifically affected by the Cdc42 deficiency. As most of the contributions of Cdc42 on cell surface dynamics and vesicle trafficking include actin polymerization as a downstream signaling event (de Curtis and Meldolesi, 2012), the finding that chemical inhibition of the actin cytoskeleton could mimic defects of Cdc42 ko DCs was not surprising. These data suggest that Cdc42 controls cellular protein contents, lysosomal integrity, and MHCII

loading by controlling actin dynamics. However, actin polymerization might be a dynamic process regulated by multiple other proteins as well. Therefore, Cdc42 deficiency does not lead to complete loss of proteins such as CTSL, the levels of which can be further decreased by chemical actin inhibition.

Most enzymes are to some extent secreted routinely as newly synthesized proenzymes (Gonzalez-Noriega et al., 1980; Hasilik and Neufeld, 1980), the majority of which still contain the mannose-6-phosphate recognition marker. This label allows subsequent uptake back into the cells via surface mannose-6-phosphate receptors (von Figura and Hasilik, 1986; Kornfeld, 1987). However, Cdc42 ko DCs secreted approximately three times more of the mature 20-kD CTSL protein as compared with wt DCs, but not its 37-kD precursor. This suggests that the proenzyme had entered the endocytic system before secretion in Cdc42 ko DCs, matured upon acidification of the vesicle, and was finally secreted from late endocytic compartments. Such enhanced secretion of lysosomal contents caused by a loss of Cdc42 in DCs was unexpected; as in other cell types, inhibition of Cdc42 has been shown to block exocytosis and secretion of vesicles, but not the opposite. For example, Cdc42 facilitates neurosecretory responses in neuroendocrine cells (Ory and Gasman, 2011) and exocytosis of membrane vesicles during neurite outgrowth in hippocampal neurons (Alberts et al., 2006). Cdc42 and other RhoGTPases control the cytoskeleton during the last step of secretory exocytosis, the discharge process. Here, in a Cdc42-dependent fashion, a thick actin layer assembles around fused vesicles, the contents of which are squeezed out of the cell. Inhibition of such a process leads to recycling by endocytosis (Nightingale et al., 2011, 2012), but not to increased secretion. According to these studies, the loss of Cdc42 function would rather reduce secretion than enhance it, at least in certain cell types. Although our study suggests a preferential loss of lysosomal proteins, we cannot formally exclude that eventually other proteins or even newly synthesized proteins are secreted as well. Additional studies are necessary to investigate the whole array of effects controlled by Cdc42. As many RhoGTPases show distinct functions in different cell types, it is possible that Cdc42 also has distinct functions during secretory processes in different cell types. In addition, the distinct secretory vesicles in neurons and DCs might require distinct modes of actin regulation by Cdc42 for efficient secretion.

Collectively, our findings suggest that Cdc42 controls several hallmarks of DC biology and function and regulates DC maturation.

Materials and methods

Mice

$Cdc42^{flx}$-Cre mice (termed Cdc42 ko) were generated by crossing mice homozygous for the *Cdc42* floxed allele ($Cdc42^{fl/fl}$ mice; Wu et al., 2006) with mice heterozygous for the *Cdc42* floxed allele, and additionally harboring the Itgax-cre (Cd11c-Cre) BAC transgene expressing Cre recombinase under the control of the CD11c promoter (Caton et al., 2007). OT-II transgenic mice express the mouse α chain and β chain T cell receptor cDNA that is specific for chicken $OVA_{323–339}$ in the context of $I\text{-}A^b$ (Barnden et al., 1998). C57BL/6 $CD45.1^+$ mice were originally obtained from The Jackson Laboratory. Mice were bred and maintained in a conventional facility at the Institute for Immunology (Munich, Germany) and used according to protocols approved by the local animal ethics committee.

Antibodies

For Western blotting, Ii protein was detected using a rat anti–mouse CD74-specific mAb clone ln-1 (BD) followed by anti–rat HRP (The Jackson Laboratory). Purified rat anti-CD107a (Biozol), goat anti-CTSS (Acris), and goat anti-CTSD and -CTSL (R&D Systems) antibodies were also used. For FACS analysis, I-Ab was detected using mouse anti-MHCII clone AF6-120.1 Alexa Fluor 647 (BD). MHCII bound to Ii was stained using mouse clone 15G4 FITC (Santa Cruz Biotechnology, Inc.). Intracellular LAMP-1 was detected using anti–CD107a-FITC or –CD107a-PE (mouse clone 1D4B; BD). CD11c was stained using Armenian hamster mAb clone N418 (eBiosciences).

DC culture and inhibitors

Primary cultures of immature DCs were generated by culturing bone marrow cells isolated from the femurs and tibiae of mice for 10–14 d in Iscove's modified Dulbecco's medium (IMDM; Sigma-Aldrich) containing 20 ng/ml granulocyte-macrophage colony stimulating factor. IMDM was further supplemented with 2 mM glutamine (Gibco), 100 U/ml penicillin, 100 µg/ml streptomycin (both PAN/Biotech), and 10% FCS (Gibco; EU Approved Origin), referred to as complete medium. Actin polymerization was inhibited by culturing wt BMDCs at days 10–12 of culture with 0.4 µg/ml LatB (EMD Millipore) or 10 µg/ml CytD (Sigma-Aldrich) overnight. Noco (Sigma-Aldrich) and ConB (Enzo Life Sciences) were added at 30 µM and 2 nM, respectively. Cells were analyzed the next day by flow cytometry. LysoTracker green DND-26 (Invitrogen) was added to the cultures at 50 nM and allowed to incorporate into lysosomes for 2 h.

Ag uptake

Immature BMDCs were harvested, resuspended at a concentration of 10^6 cells/ml in serum-free IMDM containing Alexa Fluor 647 OVA (Molecular Probes), and then incubated at 4°C or 37°C for 20 min. The reaction was stopped by washing the cells four times in ice-cold FACS buffer. Cells were then stained and analyzed by flow cytometry. Alexa OVA was titrated to visualize how much OVA was taken up by cells that were used for a T cell proliferation assay. BMDCs at day 13 of culture were incubated with various concentrations of Alexa Fluor 647 OVA for 3 h and then stimulated with 1 µg/ml LPS overnight. Cells were then stained and analyzed by flow cytometry.

T cell proliferation assay

BMDCs at day 13 of culture were pulsed with the indicated concentrations of peptide-free OVA grade VII (Sigma-Aldrich) for 3 h followed by overnight stimulation with 1 µg/ml LPS. OT-II T cells were isolated and purified as follows. Spleen and lymph nodes were harvested, and a single cell suspension was prepared. RBCs were lysed by treatment with lysis buffer (0.15 M NH_4Cl, 1 mM $KHCO_3$, and 0.1 mM Na_2EDTA, pH 7.4) for 5 min. OT-II or BALB/c T cells were enriched by negative selection using T cell isolation kits according to the manufacturer's instructions (Miltenyi Biotec). Enriched T cells were labeled with 2.5 µM carboxyfluorescein succinimidyl ester (CFSE; Molecular Probes) in PBS containing 0.03% FCS at 37°C for 10 min. Cells were co-cultured at a DC/T cell ratio of 1:20 for 3 d in round-bottom 96-well plates to enforce physical interaction of DCs and T cells, as previously published for other GTPase-deficient DCs (Benvenuti et al., 2004). T cell proliferation was analyzed by flow cytometry as CFSE dilution.

For peptide presentation, BMDCs were stimulated overnight with 1 µg/ml LPS and then incubated with the indicated concentrations of SII NFEKL or $OVA_{323–339}$ peptide (NeoMPS) for 3 h at 37°C and 5% CO_2. BMDCs were then washed three times with PBS to remove unbound peptide and co-cultured with T cells at the indicated DC/T cell ratios for 4 d. T cell proliferation was analyzed by flow cytometry as CFSE dilution.

Quantitative proteomics

Quantitative proteomics was performed for two biological replicates. Sample preparation for mass spectrometry was done as described previously (Wiśniewski et al., 2009b). In brief, 20×10^6 cells were lysed. Lysates were centrifuged at 10,000 *g* to remove insoluble cellular debris. Upon addition of five volumes of 8-M urea, one fifth of the cell lysate was subjected to filter-aided sample preparation with LysC and trypsin (Promega; Wiśniewski et al., 2009a) and fractionated into five fractions (pH 3, 5, 6, 8, and 11) using StageTip-based SAX fractionation (Wiśniewski et al., 2009a). Fractions were measured on a liquid chromatography/tandem mass spectrometry set-up coupling a Proxeon Easy nLCII (Thermo Fisher Scientific) with in-house packed 15-cm columns (75-µm internal diameter; ReproSil-Pur 120 C18-AQ, 2.4 µm; Dr. Maisch HPLC GmbH) to a mass spectrometer (LTQ Velos Orbitrap; Thermo Fisher Scientific). Peptides were separated using a 192-min binary gradient of acetonitrile in water and 0.1% formic acid at a flow rate of 300 nl/min. A TOP14 method was used for data-dependent peptide fragmentation. Data analysis, including label-free quantification, was performed using the MaxQuant software suite (version 1.5.2.8). Protein identification was performed with the integrated Andromeda algorithm searching a reviewed mouse database of UniProt also including isoforms (downloaded January 9, 2015; 24,732 entries) using standard settings of MaxQuant (Cox and Mann, 2008; Cox et al., 2011). The false discovery rate for peptide spectrum matches and proteins was adjusted to 1% by using a target and decoy strategy (reverse concatenated database). Two unique peptides per protein were required for label-free quantification. The mass spectrometry proteomics data have been deposited to the ProteomeXchange Consortium (http://proteomecentral.proteomexchange.org; Vizcaíno et al., 2014) via the PRIDE partner repository with the dataset identifier PXD001934.

DAVID clustering

Proteins that were found to be changed at least 1.5-fold in both replicates of the iquid chromatography/tandem mass spectrometry–based quantification (304) were subjected to functional annotation clustering by DAVID (Huang et al., 2009a,b). All proteins that were quantified in both replicates were used as background (2,897). Clustering was performed with the GO terms for cellular component, biological process, and molecular function (GOTERM_CC_FAT, GOTERM_BP_FAT, GOTERM_MF_FAT). The highest classification stringency was used.

Western blot

Proteins were separated by SDS-PAGE (12%). TCLs and supernatants were quantified using the Quant-iT Protein Assay kit (Molecular Probes). Equal amounts of TCLs and supernatants were loaded onto 12% SDS gels, and for TCLs, actin or tubulin was used as a loading control. After transferring to a nitrocellulose membrane, proteins were incubated with primary antibodies, washed, and incubated with secondary HRP-labeled antibodies. Then, membranes were visualized using luminescent substrate ECL (GE Healthcare). Western blot bands were quantified using ImageJ software (National Institutes of Health).

Confocal microscopy

BMDCs were seeded on poly-L-lysine–coated 12-mm round coverslips (BioCoat; BD) at a concentration of 10^6 cells/ml, allowed to settle for 1 h at 4°C, and then fixed for 5 min using 4% PFA, pH 7.4. After permeabilization with 0.1% saponin (Sigma-Aldrich), cells were stained with phalloidin–Alexa Fluor 488 (Invitrogen) and Draq5 (eBioscience). For analysis of podosomes, BMDCs were seeded on fibronectin-coated (Sigma-Aldrich) 8-well chamber slides (Lab-Tek) at a concentration of 4×10^6 cells/ml, allowed to settle for the indicated time with or without 10 ng/ml LPS at 37°C, and fixed with 4% PFA, pH 7.4. After permeabilization with 0.3% Triton X-100/PBS and 10% FCS, cells were stained with phalloidin–Alexa Fluor 488 (1:400; Invitrogen) and Draq5 (1:500; eBioscience) for 2 h at RT. For staining the colocalization of MHCII and myosin, we incubated BMDCs in media for 60 min on fibronectin-coated slides and fixed and stained them with Myosin2a (1:200; Cell Signaling Technology) and with I-E/A-E (FITC; clone M5/114; 1:400; BioLegend) at 4°C. The staining with Draq5 and goat anti–rabbit Alexa Fluor 568 (1:500; Invitrogen) followed for 2 h at RT. Coverslips were mounted on a glass slide using Fluoromount-G (SouthernBiotech) and analyzed by confocal microscopy on a confocal microscope (TCS SP5; Leica). Images were acquired at RT with a 40× 1.25 objective; image pixel size was 97.3 nm. The following color channels were used: green (488-nm excitation; 450–490-nm emission), red (568-nm excitation; 490–545-nm emission), and deep red (647-nm excitation; 640–750-nm emission). Recording was sequentially performed to avoid bleed-through. For podosome analysis, confocal images were taken at the cell–fibronectin interphase. Every confocal image was taken as one stack with fixed exposure times for both wt and Cdc42 ko samples. Images were analyzed by ImageJ software using the "bio-formats importer" plugin to open LIF files. Overlays were shown as TIFF files and transferred to Illustrator (Adobe).

mRNA isolation, reverse transcription qPCR, and primers

RNA was isolated from BMDCs using the RNeasy kit (QIAGEN) according to manufacturer's instructions, including a DNase-I on column digestion. cDNA was synthesized using the Superscript VILO cDNA Synthesis kit (Invitrogen), and qPCR was performed using the Universal ProbeLibrary mouse set (Roche). Primer sequences were designed by the Universal ProbeLibrary Assay Design Center (Roche) and were as follows: Cdc42, 5′-ACAACAAACAAATTCCCATCG-3′ and 5′-TTGCCCTGCAGTATCAAAAA-3′; CD86, 5′-CCTCCAAACCTCTCAATTTCAC-3′ and 5′-GGAGGGCCACAGTAACTGAA-3′; CD40, 5′-GAGTCAGACTAATGTCATCTGTGGTT-3′ and 5′-ACCCCGAAAATGGTGATG-3′; and CD74, 5′-CACCGAGGCTCCACCTAA-3′ and 5′-GCAGGGATGTGGCTGACT-3′. The reactions were performed on a CFX96 Real Time System and C1000 Thermal Cycler (Bio-Rad Laboratories).

Exosomes

The collection medium was complete medium previously cleared from contaminating exosomes by overnight ultracentrifugation at 100,000 *g* using a 70.1 TI rotor (Beckman Coulter). After 24 h, BMDC supernatants containing exosomes were collected, passed over a 0.2-µm filter to remove dead cells and debris, and centrifuged at 100,000 *g* for 70 min using a swinging bucket rotor (SW28; Beckman Coulter). The exosome pellet was washed three times in PBS followed by ultracentrifugation, resuspended in a small volume of PBS, and stored at −80°C. The protein concentration in BMDC TCLs and exosomes was quantified using the Quant-iT Protein Assay kit (Molecular Probes) and subjected to Western blot analysis, in which 7.5 µg of protein was loaded onto each lane.

Internalization assays

Surface Ii bound to I-Ab was stained at 4°C using purified anti–mouse 15G4 mAb. Unbound antibody was removed, and cells were allowed to internalize surface proteins at 37°C and 5% CO_2. At the indicated times, cells were transferred to 4°C and remaining 15G4 at the cell surface was stained using allophycocyanin rat anti–mouse IgG1 (BD). Cells were analyzed by flow cytometry, and relative fluorescence intensity (rFI) values of $CD11c^+$ cells were calculated using the following equation: rFI = [MFI (specific antibody) – MFI (isotype control)]/MFI (isotype control).

Statistical analysis

Statistical differences between the experimental groups were determined by Student's two-tailed *t* test. P-values of <0.05 were considered to be significant.

Online supplemental material

Fig. S1 shows defective Ag uptake and priming by Cdc42 ko DCs. Fig. S2 shows Western blot analyses of wt and Cdc42 ko DCs for CD74 and CTSD. Fig. S3 shows that treatment with actin inhibitors does not induce functional maturation of DCs to produce cytokines. Fig. S4 shows that the phenotype of Cdc42 ko DCs can be further enhanced by chemical inhibition of actin inhibitors. Fig. S5 shows analysis of exosomes by Western blot. Table S1 contains GO term analysis cellular component lysosome (GO:0005764). Table S2 shows the GO term Molecular Function Actin binding proteins (GO:0003779) analysis. Table S3 shows GO term Molecular Function Microtubule binding proteins (GO:0008017). Table S4 contains proteins that showed >1.5-fold regulation in both replicates for loading to DAVID for functional annotation clustering. Table S5 shows a list of proteins in annotation clusters with an enrichment score >1 from DAVID functional annotation analysis. Online supplemental material is available at http://www.jcb.org/cgi/content/full/jcb.201503128.DC1.

Acknowledgments

This work was supported by Deutsche Forschungsgemeinschaft grants SFB914 TPA06 and SFB1054 TPB03 to T. Brocker and SFB1181 to D. Dudziak, as well as by the German Federal Ministry of Education and the Helmholtz-Israel Cooperation in Personalized Medicine Program, the Joint Programming Neurodegenerative Diseases "Risikofaktoren und modifizierende Mechanismen bei Fronto-Temporaler Demenz," and a Frankfurt Hans and Ilse Breuer Foundation Award to S.F. Lichtenthaler.

The authors declare no competing financial interests.

A.M. Schulz, S. Stutte, N. Luckashenak, and C. Leroy planned and performed experiments and analyzed data. S. Hogl and I. Forné performed and A. Imhof and S.F. Lichtenthaler analyzed proteome data. C.H. Brakebusch provided Cdc42$^{fl/fl}$ mice; D. Dudziak provided reagents and T. Brocker planned experiments and wrote the manuscript.

Submitted: 27 March 2015
Accepted: 1 October 2015

References

Alberts, P., R. Rudge, T. Irinopoulou, L. Danglot, C. Gauthier-Rouvière, and T. Galli. 2006. Cdc42 and actin control polarized expression of TI-VAMP vesicles to neuronal growth cones and their fusion with the plasma membrane. *Mol. Biol. Cell.* 17:1194–1203. http://dx.doi.org/10.1091/mbc.E05-07-0643

Allen, W.E., D. Zicha, A.J. Ridley, and G.E. Jones. 1998. A role for Cdc42 in macrophage chemotaxis. *J. Cell Biol.* 141:1147–1157. http://dx.doi.org/10.1083/jcb.141.5.1147

Allenspach, E.J., M.P. Lemos, P.M. Porrett, L.A. Turka, and T.M. Laufer. 2008. Migratory and lymphoid-resident dendritic cells cooperate to efficiently prime naive CD4 T cells. *Immunity.* 29:795–806. http://dx.doi.org/10.1016/j.immuni.2008.08.013

Alvarez, D., E.H. Vollmann, and U.H. von Andrian. 2008. Mechanisms and consequences of dendritic cell migration. *Immunity.* 29:325–342. http://dx.doi.org/10.1016/j.immuni.2008.08.006

Anitei, M., and B. Hoflack. 2011. Bridging membrane and cytoskeleton dynamics in the secretory and endocytic pathways. *Nat. Cell Biol.* 14:11–19. http://dx.doi.org/10.1038/ncb2409

Barnden, M.J., J. Allison, W.R. Heath, and F.R. Carbone. 1998. Defective TCR expression in transgenic mice constructed using cDNA-based α- and β-chain genes under the control of heterologous regulatory elements. *Immunol. Cell Biol.* 76:34–40. http://dx.doi.org/10.1046/j.1440-1711.1998.00709.x

Beers, C., A. Burich, M.J. Kleijmeer, J.M. Griffith, P. Wong, and A.Y. Rudensky. 2005. Cathepsin S controls MHC class II-mediated antigen presentation by epithelial cells in vivo. *J. Immunol.* 174:1205–1212. http://dx.doi.org/10.4049/jimmunol.174.3.1205

Benvenuti, F., S. Hugues, M. Walmsley, S. Ruf, L. Fetler, M. Popoff, V.L. Tybulewicz, and S. Amigorena. 2004. Requirement of Rac1 and Rac2 expression by mature dendritic cells for T cell priming. *Science.* 305:1150–1153. http://dx.doi.org/10.1126/science.1099159

Bodmer, H., S. Viville, C. Benoist, and D. Mathis. 1994. Diversity of endogenous epitopes bound to MHC class II molecules limited by invariant chain. *Science.* 263:1284–1286. http://dx.doi.org/10.1126/science.7510069

Boes, M., J. Cerny, R. Massol, M. Op den Brouw, T. Kirchhausen, J. Chen, and H.L. Ploegh. 2002. T-cell engagement of dendritic cells rapidly rearranges MHC class II transport. *Nature.* 418:983–988. http://dx.doi.org/10.1038/nature01004

Brown, A.C., S. Oddos, I.M. Dobbie, J.M. Alakoskela, R.M. Parton, P. Eissmann, M.A. Neil, C. Dunsby, P.M. French, I. Davis, and D.M. Davis. 2011. Remodelling of cortical actin where lytic granules dock at natural killer cell immune synapses revealed by super-resolution microscopy. *PLoS Biol.* 9:e1001152. http://dx.doi.org/10.1371/journal.pbio.1001152

Burbage, M., S.J. Keppler, F. Gasparrini, N. Martínez-Martín, M. Gaya, C. Feest, M.C. Domart, C. Brakebusch, L. Collinson, A. Bruckbauer, and F.D. Batista. 2015. Cdc42 is a key regulator of B cell differentiation and is required for antiviral humoral immunity. *J. Exp. Med.* 212:53–72. http://dx.doi.org/10.1084/jem.20141143

Burgoyne, R.D., A. Morgan, and A.J. O'Sullivan. 1989. The control of cytoskeletal actin and exocytosis in intact and permeabilized adrenal chromaffin cells: role of calcium and protein kinase C. *Cell. Signal.* 1:323–334. http://dx.doi.org/10.1016/0898-6568(89)90051-X

Caton, M.L., M.R. Smith-Raska, and B. Reizis. 2007. Notch-RBP-J signaling controls the homeostasis of CD8-dendritic cells in the spleen. *J. Exp. Med.* 204:1653–1664. http://dx.doi.org/10.1084/jem.20062648

Chow, A., D. Toomre, W. Garrett, and I. Mellman. 2002. Dendritic cell maturation triggers retrograde MHC class II transport from lysosomes to the plasma membrane. *Nature.* 418:988–994. http://dx.doi.org/10.1038/nature01006

Cox, J., and M. Mann. 2008. MaxQuant enables high peptide identification rates, individualized p.p.b.-range mass accuracies and proteome-wide protein quantification. *Nat. Biotechnol.* 26:1367–1372. http://dx.doi.org/10.1038/nbt.1511

Cox, J., N. Neuhauser, A. Michalski, R.A. Scheltema, J.V. Olsen, and M. Mann. 2011. Andromeda: a peptide search engine integrated into the MaxQuant environment. *J. Proteome Res.* 10:1794–1805. http://dx.doi.org/10.1021/pr101065j

de Curtis, I., and J. Meldolesi. 2012. Cell surface dynamics - how Rho GTPases orchestrate the interplay between the plasma membrane and the cortical cytoskeleton. *J. Cell Sci.* 125:4435–4444. http://dx.doi.org/10.1242/jcs.108266

Dugast, M., H. Toussaint, C. Dousset, and P. Benaroch. 2005. AP2 clathrin adaptor complex, but not AP1, controls the access of the major histocompatibility complex (MHC) class II to endosomes. *J. Biol. Chem.* 280:19656–19664. http://dx.doi.org/10.1074/jbc.M501357200

Engering, A.J., M. Cella, D. Fluitsma, M. Brockhaus, E.C. Hoefsmit, A. Lanzavecchia, and J. Pieters. 1997. The mannose receptor functions as a high capacity and broad specificity antigen receptor in human dendritic cells. *Eur. J. Immunol.* 27:2417–2425. http://dx.doi.org/10.1002/eji.1830270941

Etienne-Manneville, S. 2004. Cdc42—the centre of polarity. *J. Cell Sci.* 117:1291–1300. http://dx.doi.org/10.1242/jcs.01115

Falcone, S., E. Cocucci, P. Podini, T. Kirchhausen, E. Clementi, and J. Meldolesi. 2006. Macropinocytosis: regulated coordination of endocytic and exocytic membrane traffic events. *J. Cell Sci.* 119:4758–4769. http://dx.doi.org/10.1242/jcs.03238

Faure-André, G., P. Vargas, M.I. Yuseff, M. Heuzé, J. Diaz, D. Lankar, V. Steri, J. Manry, S. Hugues, F. Vascotto, et al. 2008. Regulation of dendritic cell migration by CD74, the MHC class II-associated invariant chain. *Science.* 322:1705–1710. http://dx.doi.org/10.1126/science.1159894

Garrett, W.S., L.M. Chen, R. Kroschewski, M. Ebersold, S. Turley, S. Trombetta, J.E. Galán, and I. Mellman. 2000. Developmental control of endocytosis in dendritic cells by Cdc42. *Cell.* 102:325–334. http://dx.doi.org/10.1016/S0092-8674(00)00038-6

Gonzalez-Noriega, A., J.H. Grubb, V. Talkad, and W.S. Sly. 1980. Chloroquine inhibits lysosomal enzyme pinocytosis and enhances lysosomal enzyme

secretion by impairing receptor recycling. *J. Cell Biol.* 85:839–852. http://dx.doi.org/10.1083/jcb.85.3.839

Guo, F., C.S. Velu, H.L. Grimes, and Y. Zheng. 2009. Rho GTPase Cdc42 is essential for B-lymphocyte development and activation. *Blood.* 114:2909–2916. http://dx.doi.org/10.1182/blood-2009-04-214676

Hasilik, A., and E.F. Neufeld. 1980. Biosynthesis of lysosomal enzymes in fibroblasts. Synthesis as precursors of higher molecular weight. *J. Biol. Chem.* 255:4937–4945.

Heasman, S.J., and A.J. Ridley. 2008. Mammalian Rho GTPases: new insights into their functions from in vivo studies. *Nat. Rev. Mol. Cell Biol.* 9:690–701. http://dx.doi.org/10.1038/nrm2476

Hsing, L.C., and A.Y. Rudensky. 2005. The lysosomal cysteine proteases in MHC class II antigen presentation. *Immunol. Rev.* 207:229–241. http://dx.doi.org/10.1111/j.0105-2896.2005.00310.x

Huang, W., B.T. Sherman, and R.A. Lempicki. 2009a. Bioinformatics enrichment tools: paths toward the comprehensive functional analysis of large gene lists. *Nucleic Acids Res.* 37:1–13. http://dx.doi.org/10.1093/nar/gkn923

Huang, W., B.T. Sherman, and R.A. Lempicki. 2009b. Systematic and integrative analysis of large gene lists using DAVID bioinformatics resources. *Nat. Protoc.* 4:44–57. http://dx.doi.org/10.1038/nprot.2008.211

Inaba, K., S. Turley, T. Iyoda, F. Yamaide, S. Shimoyama, C. Reis e Sousa, R.N. Germain, I. Mellman, and R.M. Steinman. 2000. The formation of immunogenic major histocompatibility complex class II-peptide ligands in lysosomal compartments of dendritic cells is regulated by inflammatory stimuli. *J. Exp. Med.* 191:927–936. http://dx.doi.org/10.1084/jem.191.6.927

Jaksits, S., W. Bauer, E. Kriehuber, M. Zeyda, T.M. Stulnig, G. Stingl, E. Fiebiger, and D. Maurer. 2004. Lipid raft-associated GTPase signaling controls morphology and $CD8^+$ T cell stimulatory capacity of human dendritic cells. *J. Immunol.* 173:1628–1639. http://dx.doi.org/10.4049/jimmunol.173.3.1628

Kaksonen, M., C.P. Toret, and D.G. Drubin. 2006. Harnessing actin dynamics for clathrin-mediated endocytosis. *Nat. Rev. Mol. Cell Biol.* 7:404–414. http://dx.doi.org/10.1038/nrm1940

Kamon, H., T. Kawabe, H. Kitamura, J. Lee, D. Kamimura, T. Kaisho, S. Akira, A. Iwamatsu, H. Koga, M. Murakami, and T. Hirano. 2006. TRIF-GEFH1-RhoB pathway is involved in MHCII expression on dendritic cells that is critical for CD4 T-cell activation. *EMBO J.* 25:4108–4119. http://dx.doi.org/10.1038/sj.emboj.7601286

Kato, M., S. Khan, E. d'Aniello, K.J. McDonald, and D.N. Hart. 2007. The novel endocytic and phagocytic C-Type lectin receptor DCL-1/CD302 on macrophages is colocalized with F-actin, suggesting a role in cell adhesion and migration. *J. Immunol.* 179:6052–6063. http://dx.doi.org/10.4049/jimmunol.179.9.6052

Katunuma, N. 2010. Posttranslational processing and modification of cathepsins and cystatins. *J. Signal Transduct.* http://dx.doi.org/10.1155/2010/375345

Kerr, M.C., and R.D. Teasdale. 2009. Defining macropinocytosis. *Traffic.* 10:364–371. http://dx.doi.org/10.1111/j.1600-0854.2009.00878.x

Kleijmeer, M.J., S. Morkowski, J.M. Griffith, A.Y. Rudensky, and H.J. Geuze. 1997. Major histocompatibility complex class II compartments in human and mouse B lymphoblasts represent conventional endocytic compartments. *J. Cell Biol.* 139:639–649. http://dx.doi.org/10.1083/jcb.139.3.639

Kornfeld, S. 1987. Trafficking of lysosomal enzymes. *FASEB J.* 1:462–468.

Lämmermann, T., B.L. Bader, S.J. Monkley, T. Worbs, R. Wedlich-Söldner, K. Hirsch, M. Keller, R. Förster, D.R. Critchley, R. Fässler, and M. Sixt. 2008. Rapid leukocyte migration by integrin-independent flowing and squeezing. *Nature.* 453:51–55. http://dx.doi.org/10.1038/nature06887

Landsverk, O.J., O. Bakke, and T.F. Gregers. 2009. MHC II and the endocytic pathway: regulation by invariant chain. *Scand. J. Immunol.* 70:184–193. http://dx.doi.org/10.1111/j.1365-3083.2009.02301.x

Lautwein, A., T. Burster, A.M. Lennon-Duménil, H.S. Overkleeft, E. Weber, H. Kalbacher, and C. Driessen. 2002. Inflammatory stimuli recruit cathepsin activity to late endosomal compartments in human dendritic cells. *Eur. J. Immunol.* 32:3348–3357. http://dx.doi.org/10.1002/1521-4141(200212)32:12<3348::AID-IMMU3348>3.0.CO;2-S

Luckashenak, N., A. Wähe, K. Breit, C. Brakebusch, and T. Brocker. 2013. Rho-family GTPase Cdc42 controls migration of Langerhans cells in vivo. *J. Immunol.* 190:27–35. http://dx.doi.org/10.4049/jimmunol.1201082

Lukacs-Kornek, V., and S.J. Turley. 2008. Immunology. Chaperone puts the brakes on. *Science.* 322:1640–1641. http://dx.doi.org/10.1126/science.1168103

McCormick, P.J., J.A. Martina, and J.S. Bonifacino. 2005. Involvement of clathrin and AP-2 in the trafficking of MHC class II molecules to antigen-processing compartments. *Proc. Natl. Acad. Sci. USA.* 102:7910–7915. http://dx.doi.org/10.1073/pnas.0502206102

McGavin, M.K., K. Badour, L.A. Hardy, T.J. Kubiseski, J. Zhang, and K.A. Siminovitch. 2001. The intersectin 2 adaptor links Wiskott Aldrich Syndrome protein (WASp)-mediated actin polymerization to T cell antigen receptor endocytosis. *J. Exp. Med.* 194:1777–1787. http://dx.doi.org/10.1084/jem.194.12.1777

Merad, M., P. Sathe, J. Helft, J. Miller, and A. Mortha. 2013. The dendritic cell lineage: ontogeny and function of dendritic cells and their subsets in the steady state and the inflamed setting. *Annu. Rev. Immunol.* 31:563–604. http://dx.doi.org/10.1146/annurev-immunol-020711-074950

Neefjes, J., M.L. Jongsma, P. Paul, and O. Bakke. 2011. Towards a systems understanding of MHC class I and MHC class II antigen presentation. *Nat. Rev. Immunol.* 11:823–836. http://dx.doi.org/10.1038/nri3084

Nevins, A.K., and D.C. Thurmond. 2003. Glucose regulates the cortical actin network through modulation of Cdc42 cycling to stimulate insulin secretion. *Am. J. Physiol. Cell Physiol.* 285:C698–C710. http://dx.doi.org/10.1152/ajpcell.00093.2003

Niedergang, F., and P. Chavrier. 2004. Signaling and membrane dynamics during phagocytosis: many roads lead to the phagos(R)ome. *Curr. Opin. Cell Biol.* 16:422–428. http://dx.doi.org/10.1016/j.ceb.2004.06.006

Nightingale, T.D., I.J. White, E.L. Doyle, M. Turmaine, K.J. Harrison-Lavoie, K.F. Webb, L.P. Cramer, and D.F. Cutler. 2011. Actomyosin II contractility expels von Willebrand factor from Weibel-Palade bodies during exocytosis. *J. Cell Biol.* 194:613–629. http://dx.doi.org/10.1083/jcb.201011119

Nightingale, T.D., D.F. Cutler, and L.P. Cramer. 2012. Actin coats and rings promote regulated exocytosis. *Trends Cell Biol.* 22:329–337. http://dx.doi.org/10.1016/j.tcb.2012.03.003

Nobes, C.D., and A. Hall. 1999. Rho GTPases control polarity, protrusion, and adhesion during cell movement. *J. Cell Biol.* 144:1235–1244. http://dx.doi.org/10.1083/jcb.144.6.1235

Orci, L., K.H. Gabbay, and W.J. Malaisse. 1972. Pancreatic beta-cell web: its possible role in insulin secretion. *Science.* 175:1128–1130. http://dx.doi.org/10.1126/science.175.4026.1128

Ory, S., and S. Gasman. 2011. Rho GTPases and exocytosis: what are the molecular links? *Semin. Cell Dev. Biol.* 22:27–32. http://dx.doi.org/10.1016/j.semcdb.2010.12.002

Platt, C.D., J.K. Ma, C. Chalouni, M. Ebersold, H. Bou-Reslan, R.A. Carano, I. Mellman, and L. Delamarre. 2010. Mature dendritic cells use endocytic receptors to capture and present antigens. *Proc. Natl. Acad. Sci. USA.* 107:4287–4292. http://dx.doi.org/10.1073/pnas.0910609107

Pulecio, J., J. Petrovic, F. Prete, G. Chiaruttini, A.M. Lennon-Dumenil, C. Desdouets, S. Gasman, O.R. Burrone, and F. Benvenuti. 2010. Cdc42-mediated MTOC polarization in dendritic cells controls targeted delivery of cytokines at the immune synapse. *J. Exp. Med.* 207:2719–2732. http://dx.doi.org/10.1084/jem.20100007

Qualmann, B., and H. Mellor. 2003. Regulation of endocytic traffic by Rho GTPases. *Biochem. J.* 371:233–241. http://dx.doi.org/10.1042/bj20030139

Santambrogio, L., I. Potolicchio, S.P. Fessler, S.H. Wong, G. Raposo, and J.L. Strominger. 2005. Involvement of caspase-cleaved and intact adaptor protein 1 complex in endosomal remodeling in maturing dendritic cells. *Nat. Immunol.* 6:1020–1028. http://dx.doi.org/10.1038/ni1250

Schafer, D.A. 2002. Coupling actin dynamics and membrane dynamics during endocytosis. *Curr. Opin. Cell Biol.* 14:76–81. http://dx.doi.org/10.1016/S0955-0674(01)00297-6

Shurin, G.V., R.L. Ferris, I.L. Tourkova, L. Perez, A. Lokshin, L. Balkir, B. Collins, G.S. Chatta, and M.R. Shurin. 2005a. Loss of new chemokine CXCL14 in tumor tissue is associated with low infiltration by dendritic cells (DC), while restoration of human CXCL14 expression in tumor cells causes attraction of DC both in vitro and in vivo. *J. Immunol.* 174:5490–5498. http://dx.doi.org/10.4049/jimmunol.174.9.5490

Shurin, G.V., I.L. Tourkova, G.S. Chatta, G. Schmidt, S. Wei, J.Y. Djeu, and M.R. Shurin. 2005b. Small rho GTPases regulate antigen presentation in dendritic cells. *J. Immunol.* 174:3394–3400. http://dx.doi.org/10.4049/jimmunol.174.6.3394

Smyth, C., G. Logan, R.P. Weinberger, P.B. Rowe, I.E. Alexander, and J.A. Smythe. 1998. Identification of a dynamic intracellular reservoir of CD86 protein in peripheral blood monocytes that is not associated with the Golgi complex. *J. Immunol.* 160:5390–5396.

Smyth, C.M., G. Logan, R. Boadle, P.B. Rowe, J.A. Smythe, and I.E. Alexander. 2005. Differential subcellular localization of CD86 in human PBMC-derived macrophages and DCs, and ultrastructural characterization by immuno-electron microscopy. *Int. Immunol.* 17:123–132. http://dx.doi.org/10.1093/intimm/dxh193

Tewari, M.K., G. Sinnathamby, D. Rajagopal, and L.C. Eisenlohr. 2005. A cytosolic pathway for MHC class II-restricted antigen processing that is

proteasome and TAP dependent. *Nat. Immunol.* 6:287–294. http://dx.doi.org/10.1038/ni1171

Trombetta, E.S., and I. Mellman. 2005. Cell biology of antigen processing in vitro and in vivo. *Annu. Rev. Immunol.* 23:975–1028. http://dx.doi.org/10.1146/annurev.immunol.22.012703.104538

Turk, V., V. Stoka, O. Vasiljeva, M. Renko, T. Sun, B. Turk, and D. Turk. 2012. Cysteine cathepsins: from structure, function and regulation to new frontiers. *Biochim. Biophys. Acta.* 1824:68–88. http://dx.doi.org/10.1016/j.bbapap.2011.10.002

Tybulewicz, V.L., and R.B. Henderson. 2009. Rho family GTPases and their regulators in lymphocytes. *Nat. Rev. Immunol.* 9:630–644. http://dx.doi.org/10.1038/nri2606

van Niel, G., R. Wubbolts, T. Ten Broeke, S.I. Buschow, F.A. Ossendorp, C.J. Melief, G. Raposo, B.W. van Balkom, and W. Stoorvogel. 2006. Dendritic cells regulate exposure of MHC class II at their plasma membrane by oligoubiquitination. *Immunity.* 25:885–894. http://dx.doi.org/10.1016/j.immuni.2006.11.001

Vizcaíno, J.A., E.W. Deutsch, R. Wang, A. Csordas, F. Reisinger, D. Ríos, J.A. Dianes, Z. Sun, T. Farrah, N. Bandeira, et al. 2014. ProteomeXchange provides globally coordinated proteomics data submission and dissemination. *Nat. Biotechnol.* 32:223–226. http://dx.doi.org/10.1038/nbt.2839

von Figura, K., and A. Hasilik. 1986. Lysosomal enzymes and their receptors. *Annu. Rev. Biochem.* 55:167–193. http://dx.doi.org/10.1146/annurev.bi.55.070186.001123

Wang, L., and Y. Zheng. 2007. Cell type-specific functions of Rho GTPases revealed by gene targeting in mice. *Trends Cell Biol.* 17:58–64. http://dx.doi.org/10.1016/j.tcb.2006.11.009

Watts, C., and S. Amigorena. 2000. Antigen traffic pathways in dendritic cells. *Traffic.* 1:312–317. http://dx.doi.org/10.1034/j.1600-0854.2000.010404.x

West, M.A., A.R. Prescott, E.L. Eskelinen, A.J. Ridley, and C. Watts. 2000. Rac is required for constitutive macropinocytosis by dendritic cells but does not control its downregulation. *Curr. Biol.* 10:839–848. http://dx.doi.org/10.1016/S0960-9822(00)00595-9

West, M.A., R.P. Wallin, S.P. Matthews, H.G. Svensson, R. Zaru, H.G. Ljunggren, A.R. Prescott, and C. Watts. 2004. Enhanced dendritic cell antigen capture via toll-like receptor-induced actin remodeling. *Science.* 305:1153–1157. http://dx.doi.org/10.1126/science.1099153

Wiśniewski, J.R., A. Zougman, and M. Mann. 2009a. Combination of FASP and StageTip-based fractionation allows in-depth analysis of the hippocampal membrane proteome. *J. Proteome Res.* 8:5674–5678. http://dx.doi.org/10.1021/pr900748n

Wiśniewski, J.R., A. Zougman, N. Nagaraj, and M. Mann. 2009b. Universal sample preparation method for proteome analysis. *Nat. Methods.* 6:359–362. http://dx.doi.org/10.1038/nmeth.1322

Wollman, R., and T. Meyer. 2012. Coordinated oscillations in cortical actin and Ca^{2+} correlate with cycles of vesicle secretion. *Nat. Cell Biol.* 14:1261–1269. http://dx.doi.org/10.1038/ncb2614

Wraight, C.J., P. van Endert, P. Möller, J. Lipp, N.R. Ling, I.C. MacLennan, N. Koch, and G. Moldenhauer. 1990. Human major histocompatibility complex class II invariant chain is expressed on the cell surface. *J. Biol. Chem.* 265:5787–5792.

Wu, X., F. Quondamatteo, T. Lefever, A. Czuchra, H. Meyer, A. Chrostek, R. Paus, L. Langbein, and C. Brakebusch. 2006. Cdc42 controls progenitor cell differentiation and β-catenin turnover in skin. *Genes Dev.* 20:571–585. http://dx.doi.org/10.1101/gad.361406

Yuseff, M.I., A. Reversat, D. Lankar, J. Diaz, I. Fanget, P. Pierobon, V. Randrian, N. Larochette, F. Vascotto, C. Desdouets, et al. 2011. Polarized secretion of lysosomes at the B cell synapse couples antigen extraction to processing and presentation. *Immunity.* 35:361–374. http://dx.doi.org/10.1016/j.immuni.2011.07.008

Zhang, J., A. Shehabeldin, L.A. da Cruz, J. Butler, A.K. Somani, M. McGavin, I. Kozieradzki, A.O. dos Santos, A. Nagy, S. Grinstein, et al. 1999. Antigen receptor-induced activation and cytoskeletal rearrangement are impaired in Wiskott-Aldrich syndrome protein-deficient lymphocytes. *J. Exp. Med.* 190:1329–1342. http://dx.doi.org/10.1084/jem.190.9.1329

Zitvogel, L., A. Regnault, A. Lozier, J. Wolfers, C. Flament, D. Tenza, P. Ricciardi-Castagnoli, G. Raposo, and S. Amigorena. 1998. Eradication of established murine tumors using a novel cell-free vaccine: dendritic cell-derived exosomes. *Nat. Med.* 4:594–600. http://dx.doi.org/10.1038/nm0598-594